REPORT DOCUMENTATION PAGE

Form Approved OMB No. 0704-0188

1. REPORT DATE *(DD-MM-YYYY)* 13-10-2011	**2. REPORT TYPE** Seminar Presentation	**3. DATES COVERED** *(From - To)*

4. TITLE AND SUBTITLE

Effect of Gas Injection on Transition in Hypervelocity Boundary Layers

5a. CONTRACT NUMBER

5b. GRANT NUMBER

5c. PROGRAM ELEMENT NUMBER

6. AUTHOR(S)

Ivett Leyva, Joseph .S. Jewell, Nicholaus J. Parziale, Joseph E. Sheperd and Hans Hornung (GALCIT, Caltech), Ross Wagnild and Prof. Graham Candler (University of Minnesota)

5d. PROJECT NUMBER

5f. WORK UNIT NUMBER
23070725

7. PERFORMING ORGANIZATION NAME(S) AND ADDRESS(ES)

Air Force Research Laboratory (AFMC)
AFRL/RZSA
10 E. Saturn Blvd.
Edwards AFB CA 93524-7680

8. PERFORMING ORGANIZATION REPORT NUMBER

AFRL-RZ-ED-VG-2011-404

9. SPONSORING / MONITORING AGENCY NAME(S) AND ADDRESS(ES)

Air Force Research Laboratory (AFMC)
AFRL/RZS
5 Pollux Drive
Edwards AFB CA 93524-7048

10. SPONSOR/MONITOR'S ACRONYM(S)

11. SPONSOR/MONITOR'S NUMBER(S)
AFRL-RZ-ED-VG-2011-404

12. DISTRIBUTION / AVAILABILITY STATEMENT

Approved for public release; distribution unlimited (PA #11876).

13. SUPPLEMENTARY NOTES
For presentation at an invited seminar at Texas A&M University, 19 Oct 2011.

14. ABSTRACT
A novel method to delay transition in hypervelocity flows in air over slender bodies by injecting CO_2 into the boundary layer is presented. The dominant transition mechanism in hypersonic flow is the inviscid second (Mack) mode, which is associated with acoustic disturbances which are trapped and amplified inside the boundary layer [8]. In dissociated CO_2-rich flows, nonequilibrium molecular vibration damps the acoustic instability, and for the high-temperature, high-pressure conditions associated with hypervelocity flows, the effect is most pronounced in the frequency bands amplified by the second mode [3]. Experimental data were obtained in Caltech's T5 reflected shock tunnel. The experimental model was a 5 degree half-angle sharp cone instrumented with 80 thermocouples, providing heat transfer measurements from which transition locations were from turbulent intermittency based upon laminar and turbulent heat flux correlations. An appropriate injector was designed and fabricated, and the efficacy of injecting CO_2 in delaying transition was gauged at various mass flow rates, and compared with both no injection and chemically inert Argon injection cases. Argon was chosen for its similar density to CO_2. At an enthalpy of approximately 10 MJ/kg (Eckert's reference temperature $T\_$ = 2550 K), transition delays in terms of Reynolds number were documented. For Argon injection cases at similar mass flow rates, transition is promoted.
.

15. SUBJECT TERMS

16. SECURITY CLASSIFICATION OF:			**17. LIMITATION OF ABSTRACT**	**18. NUMBER OF PAGES**	**19a. NAME OF RESPONSIBLE PERSON**
					Dr. Ivett A. Leyva
a. REPORT	**b. ABSTRACT**	**c. THIS PAGE**			**19b. TELEPHONE NUMBER** *(include area code)*
Unclassified	**Unclassified**	**Unclassified**	SAR	68	N/A

Effect of gas injection on transition in hypervelocity boundary layers

Ivett A. Leyva

AFRL/RZSA, Edwards Air Force Base, CA

Joseph S. Jewell, Nicholaus J. Parziale, Joseph E. Shepherd, Hans Hornung

GALCIT, Caltech, Pasadena, CA

Ross Wagnild, Prof. Graham Candler

University of Minnesota, Minneapolis, MN

AFOSR PM: John Schmisseur

AFOSR Grant F49620-IHOUSE07E0000

October 20, 2011

Delay transition using non-equilibrium CO_2

PROBLEM: **In hypersonic flight, heating loads are typically a dominant design factor**

Turbulent heat transfer rates can be about an order of magnitude higher than laminar rates at hypersonic Mach numbers

A reduction in heating loads by keeping the boundary layer laminar longer means less thermal protection needed and hence less weight to carry, or conversely more payload deliverable for a given thrust.

OBJECTIVE: **Delay transition from laminar to turbulent flow in the boundary layer of a slender hypersonic body by using nonequilibrium CO_2**

Transition in high Mach numbers occurs through the Mack mode – amplification of acoustic waves traveling in the boundary layer

Molecular vibration and dissociation damp acoustic waves

At relevant conditions, CO_2 absorbs most energy at the frequencies most strongly amplified by 2^{nd} (Mack) mode

Inject CO_2 to delay transition in air flows of interest

Background

- **Experimental data show that transition is delayed for CO_2 flows compared with N_2 and air flows for a given stagnation enthalpy, h_o**
- **These observations point to a second mode transition (or Mack mode) for the conditions studied as well as to the importance of non-equilibrium effects of CO_2 on stabilizing the flow**

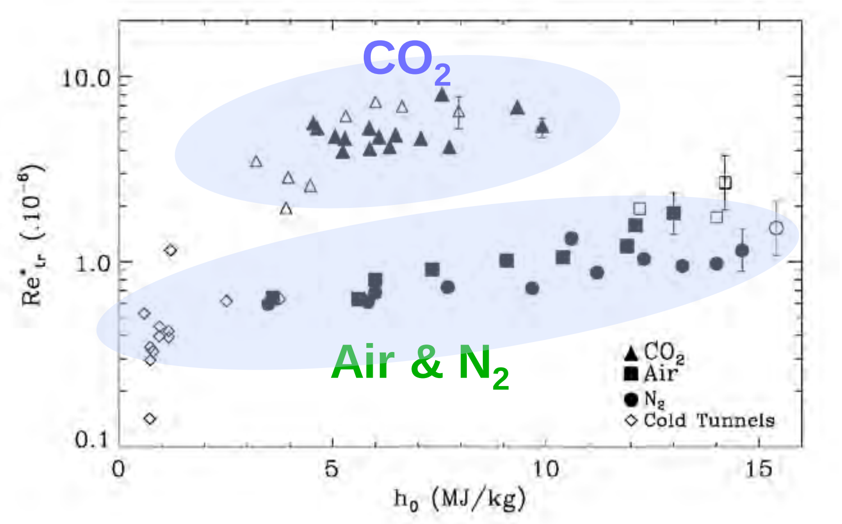

CO_2 Transition Re* is about 5X that of Air and N2

From Hornung, H.G., Adam, P.H., Germain, P., Fujii, K., Rasheed, A., "On transition and transition control in hypervelocity flows," *Proceedings of the Ninth Asian Congress of Fluid Mechanics*, 2002

Background

Computations show that when pure CO_2 is in vibrational and chemical non-equilibrium, these relaxation processes absorb energy from acoustic disturbances in the boundary layer whose growth is responsible for transition in hypervelocity flows

Confirms trends seen in experiments where CO_2 exhibits delayed transition with respect to Air or N_2 for h_0~5-10MJ/kg

For air – no effect from vibrational relaxation and chemical reactions on stabilizing the boundary layer

For CO_2 – vibrational relaxation and chemical reactions stabilizes the boundary layer

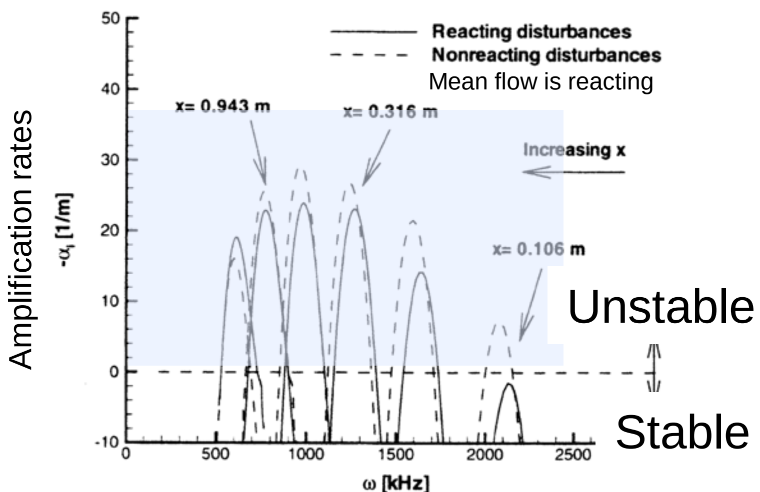

Air

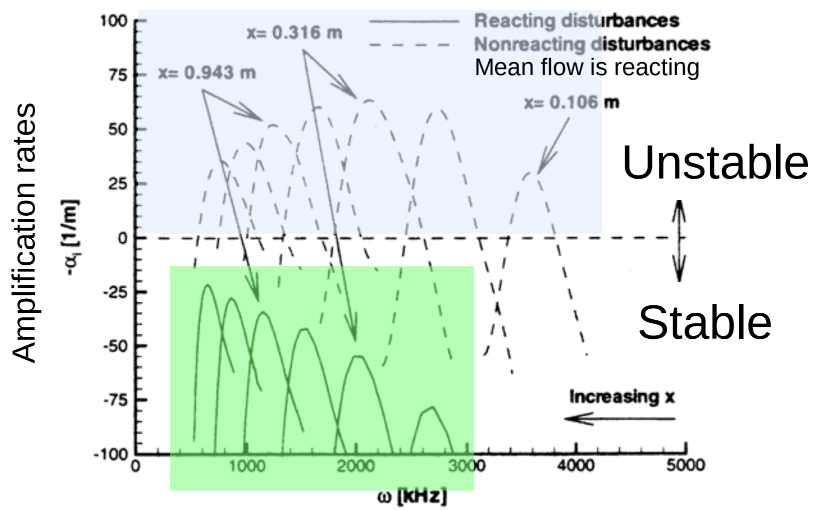

CO_2

From Johnson, H.B., Seipp, T.G., Candler, G.V., "Numerical study of hypersonic reacting boundary layer transition on cones," *Physics of Fluids, 10 (10): 2676-2685 Oct. 1998.*

Background

- **Computed acoustic absorption rates (open symbols) – Fujii et. al**
- **Computed acoustic amplification rates (solid symbols) – after Reshotko/Beckwith and Mack**
- **For CO_2 the broad sound absorption curve peak coincides with the amplification peaks**
- **This coincidence is most pronounced at enthalpies of ~10 MJ/kg**

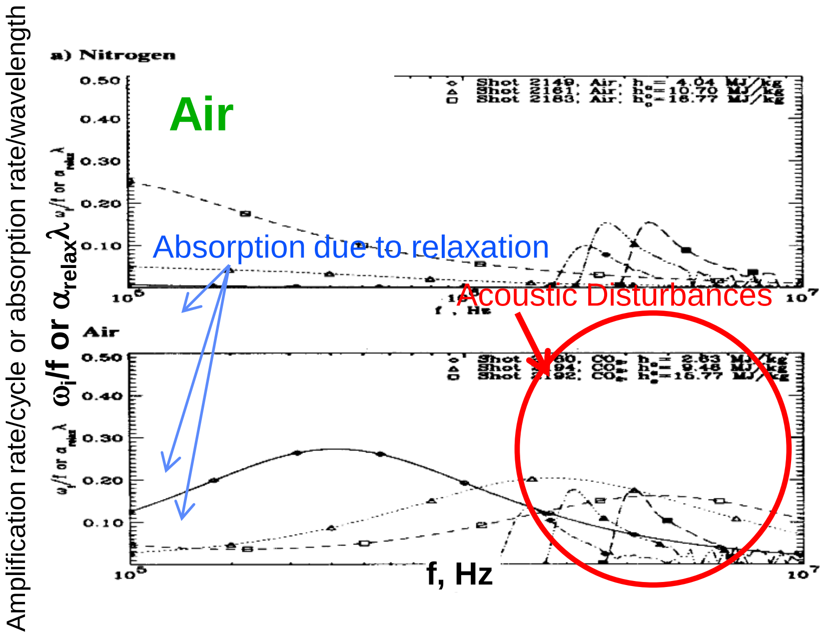

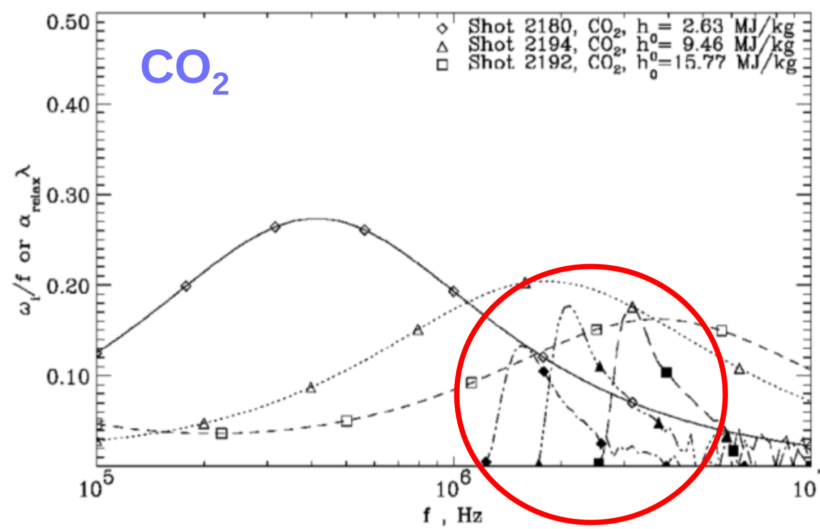

From: Fujii, K., Hornung, H.G, "Experinmental Investigation of High-Enthalpy Effects on Attachment-Line Boundary Layer Transition," AIAA Journal, Vol. 41, No. 7, July 2003

Facility: T5 Hypervelocity Shock Tunnel

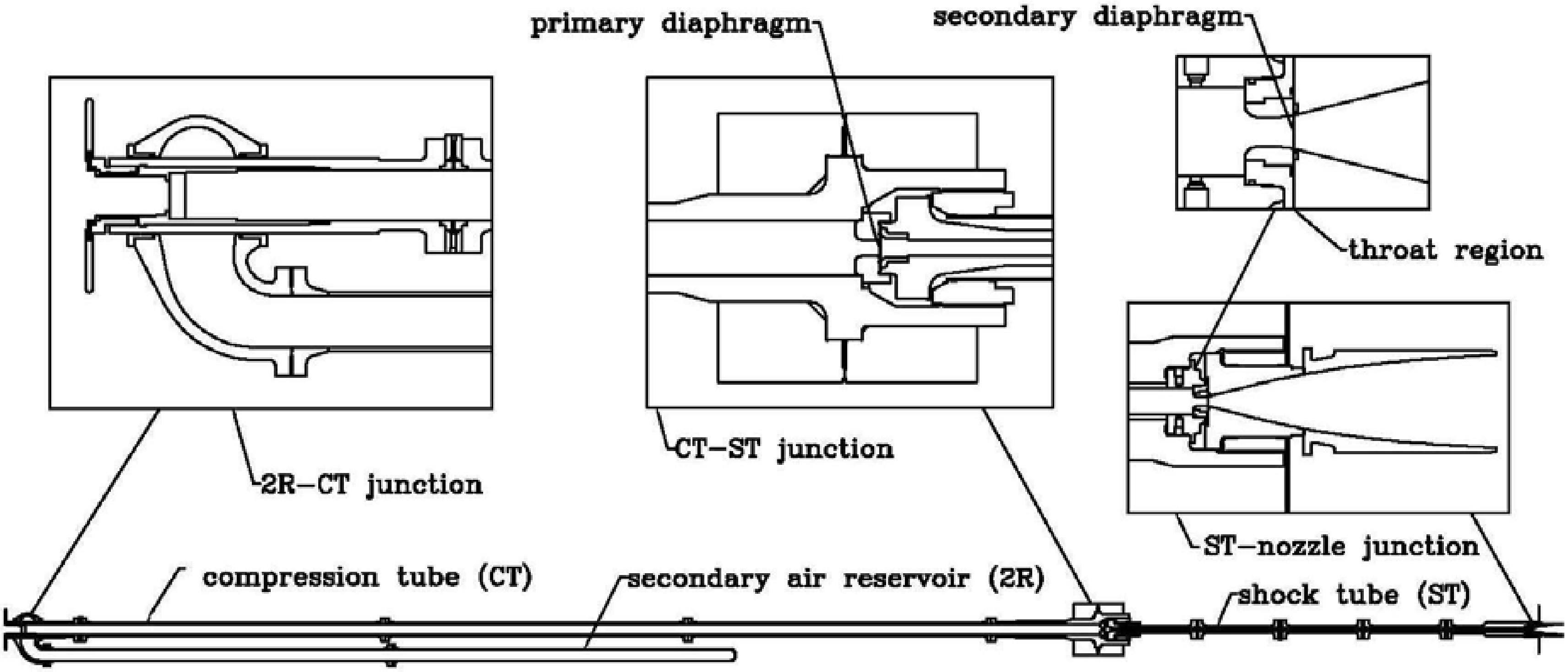

Impulse Facility, test time in the order of ms, but high stagnation enthalpies and pressures

Free-stream mixtures with CO_2

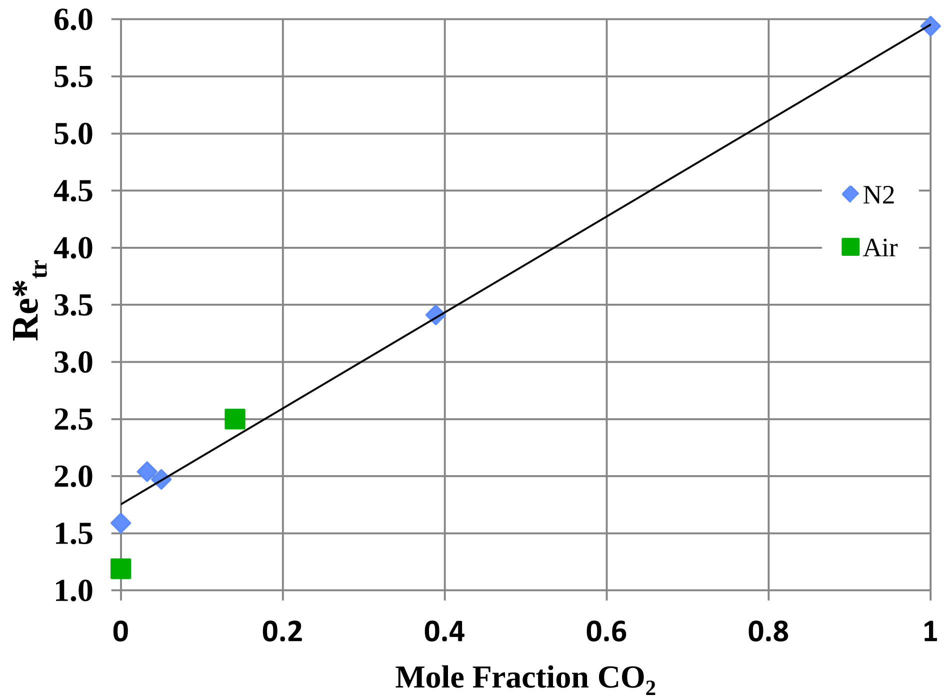

From Leyva, IA, Laurence, S, Beierholm, AK-W, Hornung, HG, Wagnild, R, and Candler, G, "Transition delay in hypervelocity boundary layers by means of CO2/acoustic instability interactions," *47th AIAA Aerospace Sciences Meeting,* AIAA 2009-1287.

Porous Injector

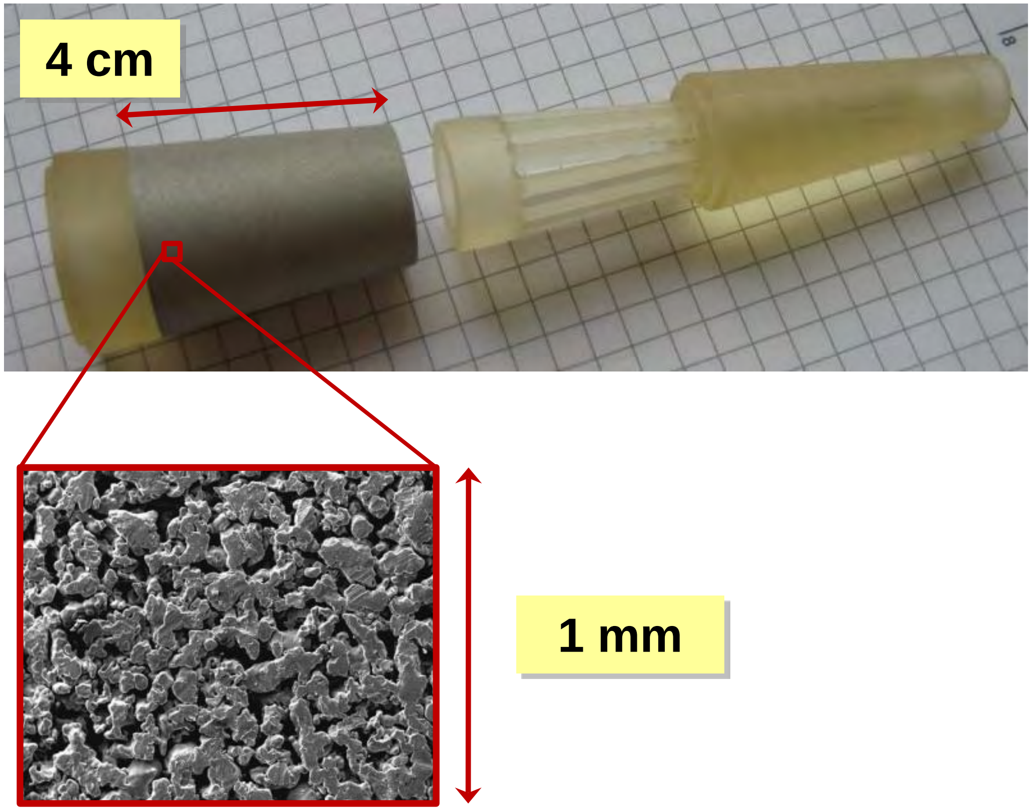

Porous injector section
Sintered 316LL Stainless Steel
10 μm media grade

Porous Injector Rationale

- Move to a transpiration-like approach instead of discrete jets
- High velocity jets disturbed the boundary layer – penetrate to shock layer
- Need lower flow penetration into the boundary layer
- Can achieve same flow rates as with jets ~ 0-50 g/s

Porous Injector Results (10 MJ/kg)

10-micron Porous Injector (**Ar** injection at 3.7 grams/sec)

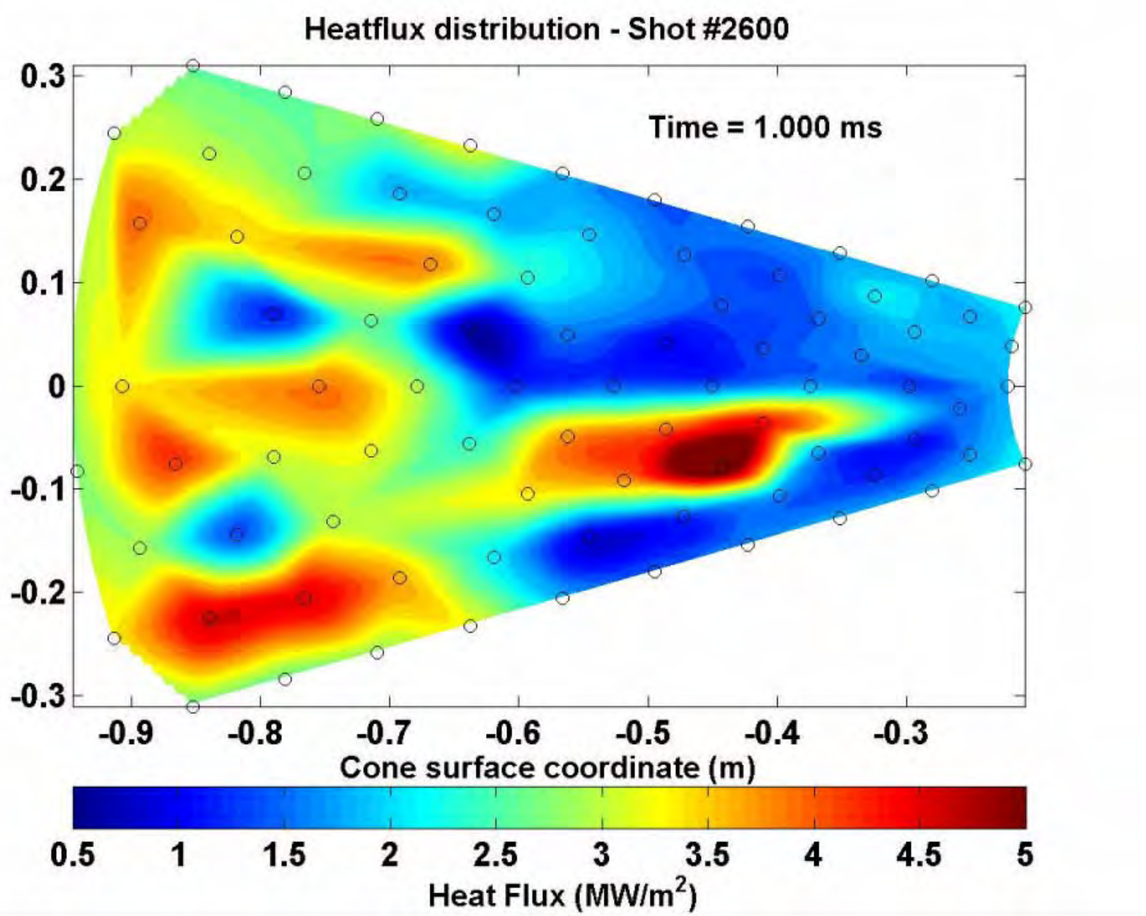

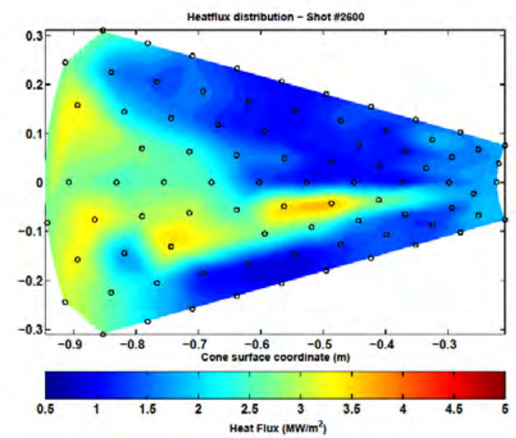

Average over test time

(1.500 – 2.100 ms)

Porous Injector Results (10 MJ/kg)

10-micron Porous Injector (no injection)

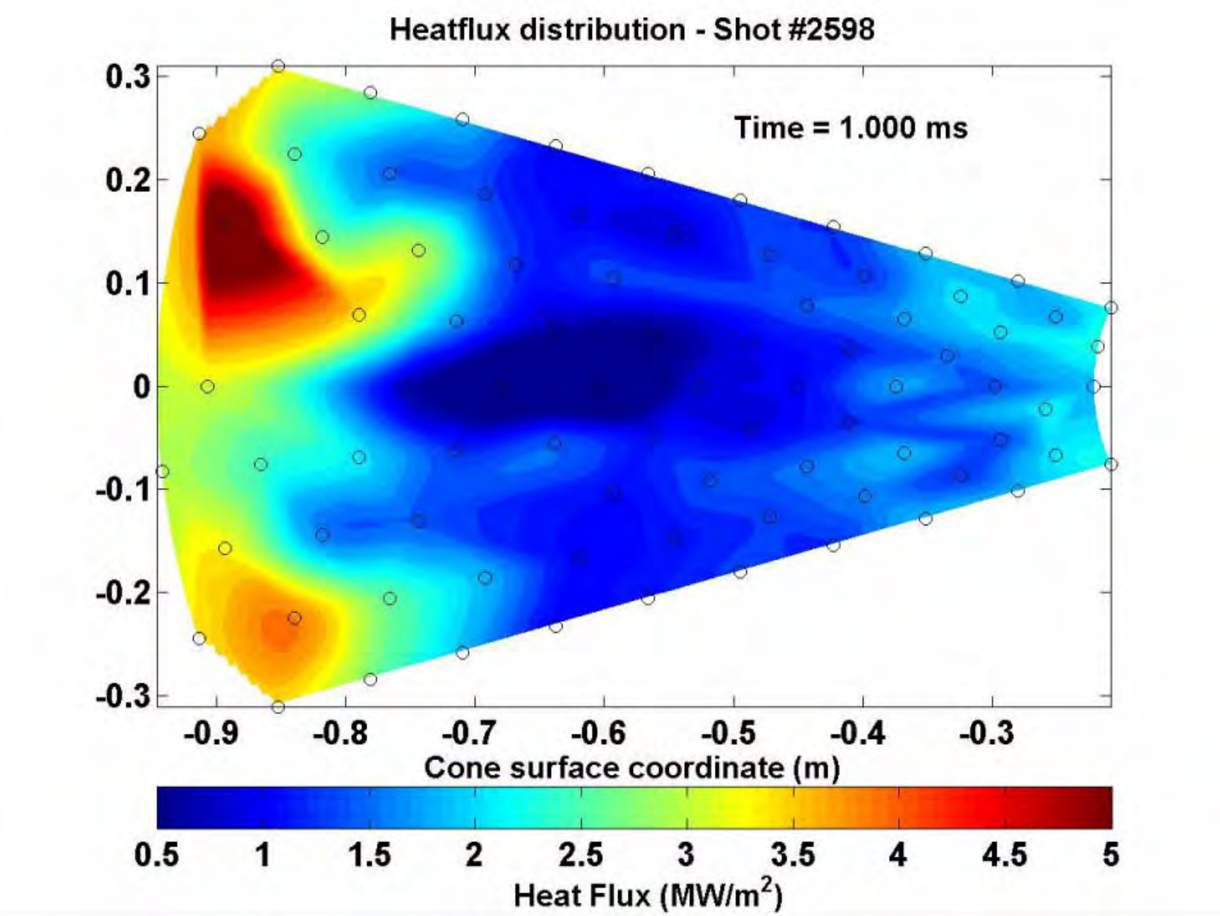

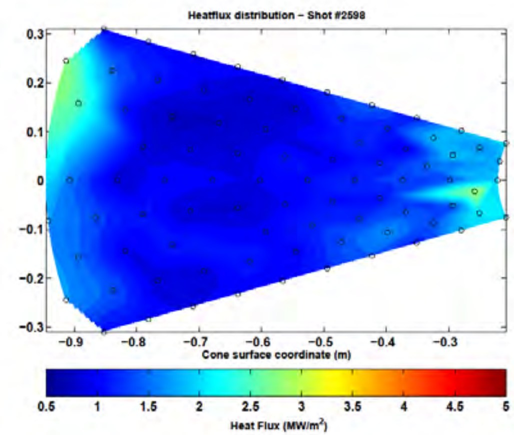

Average over test time

(1.500 – 2.100 ms)

Porous Injector Results (10 MJ/kg)

10-micron Porous Injector (**CO_2** injection at 3.7 grams/sec)

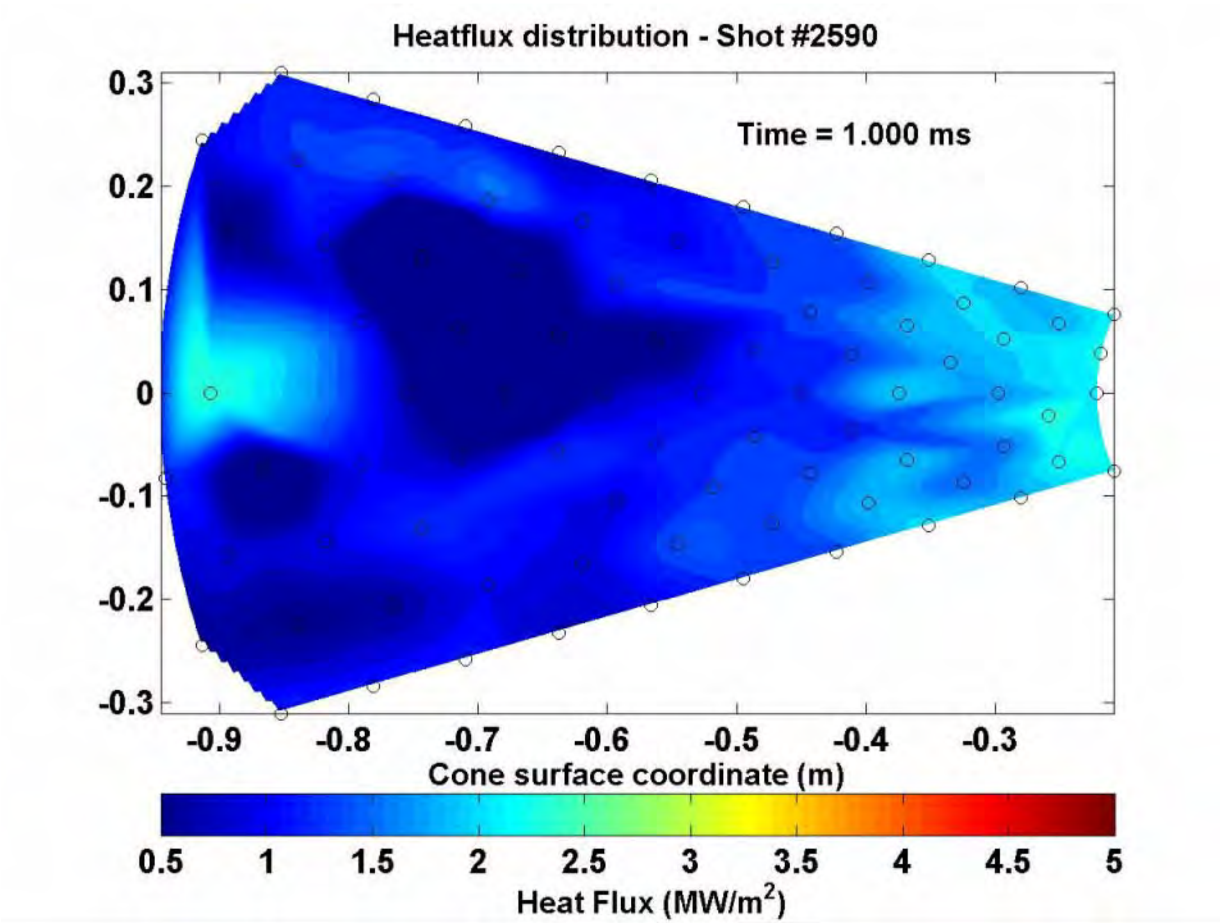

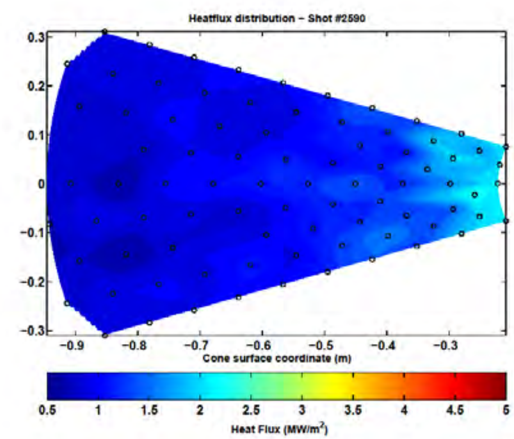

Average over test time

(1.500 – 2.100 ms)

Porous Injector Results 1/2

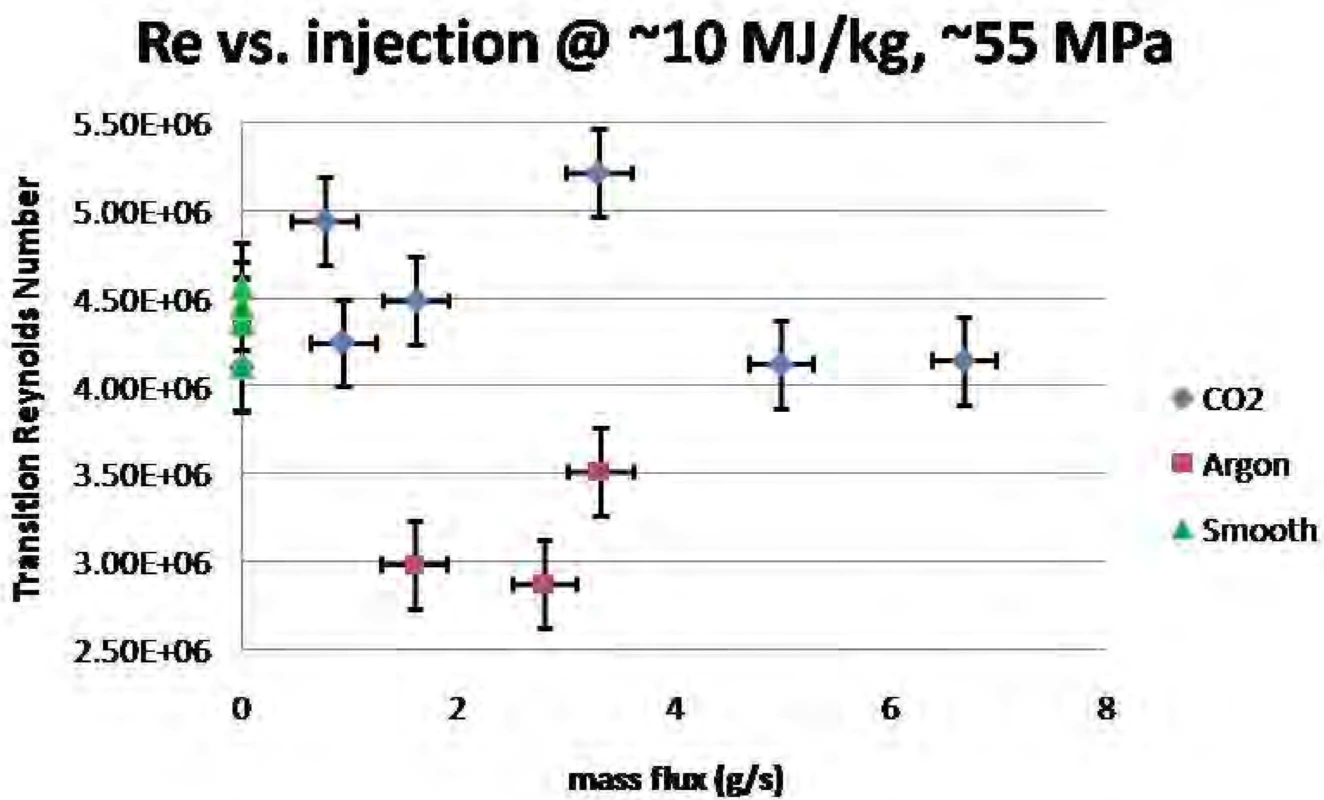

Data reduction: Average Heat Transfer Method

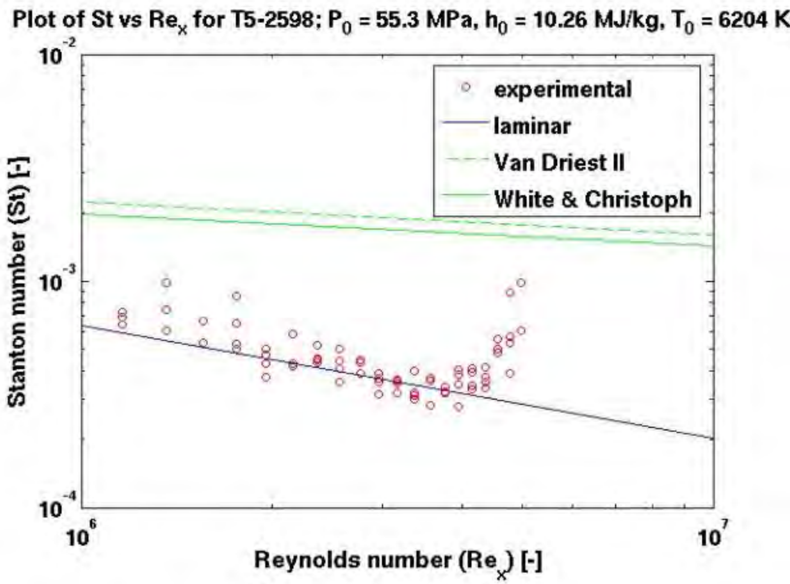

No injection: porous section

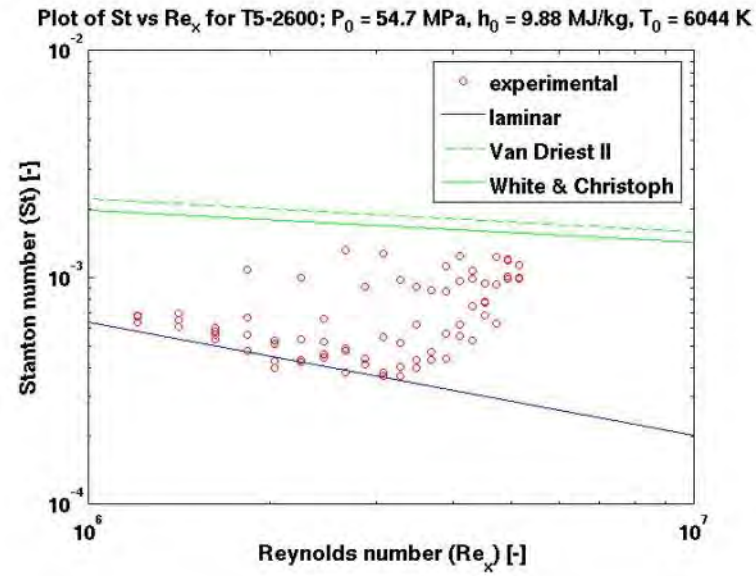

Argon Injection: 3.7 g/s

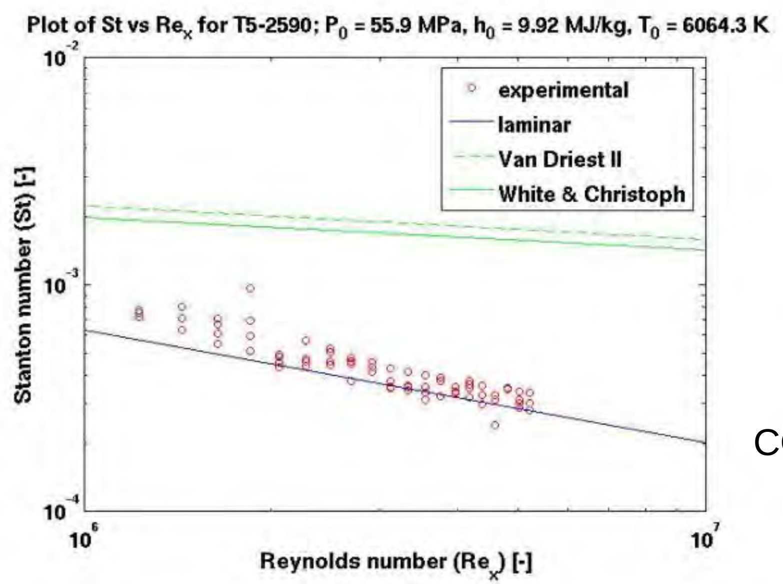

CO_2 injection: 3.7 g/s

Data Reduction: Intermittency Method

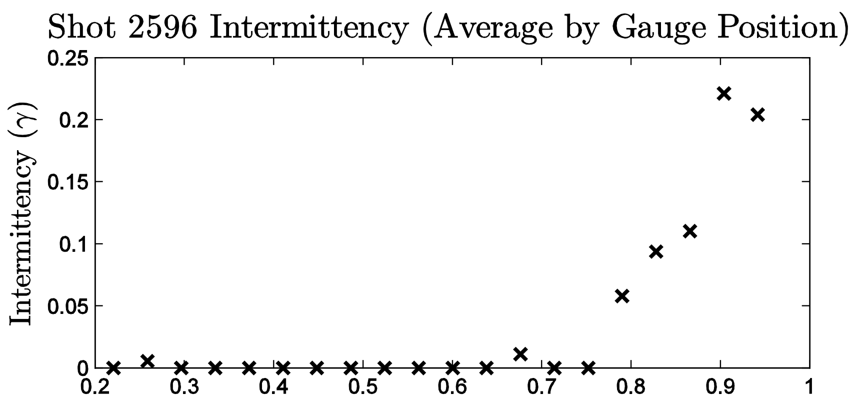

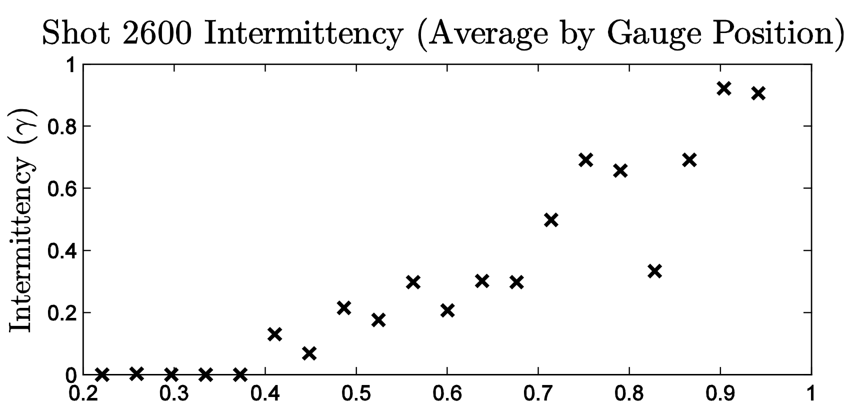

Turbulent intermittency

- Mee D.J. and Goyne C.P. (1996) Turbulent spots in boundary layers in a free-piston shock tunnel flow. Shock Waves, Vol. 6, No. 6:337–343.
- Narasimha R. (1985) The Laminar-Turbulent Transition Zone in the Boundary Layer. Progress in Aerospace Sciences, Vol. 22, 29–80.

Alternate method to determine transition location

Porous Injector Results (10 MJ/kg)

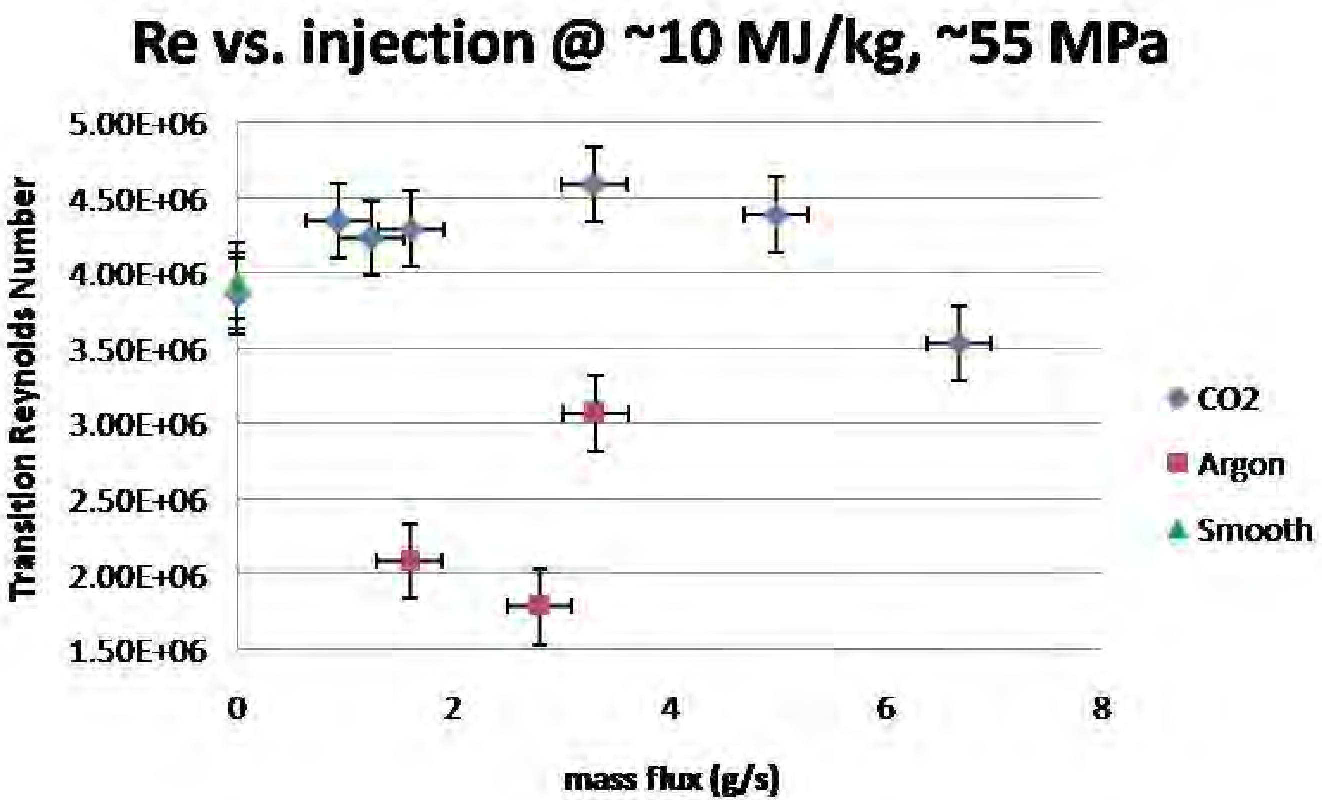

Summary of results (intermittency method)

Theoretical Injection

- **Free-stream gas is Nitrogen**
- **Different injection geometry**
  - **5 degree cone, transpiration from 10 to 90 cm on the cone**

Stagnation Conditions		Free-stream Conditions	
Pressure (MPa)	55.0	Density (kg/m^3)	0.051855
Temperature (K)	6958	Temperature (K)	925.5
Entalpy (MJ/kg)	9.39	Velocity (m/s)	4039.7

- **Injection based on profile suggested by Malik***
  - **mdot based on edge conditions and parameter, f_w**
- **For these cases, f_w held constant**
  - **Mass flux decreases down the length of the cone**

$$f_w = \frac{\sqrt{2\,\mathrm{Re}_x}\,\rho_w v_w}{\rho_e v_e}$$

f_w	Mass Flux (g/s)
0.05	1.24
0.1	2.47
0.2	4.96
0.3	7.43
0.4	9.92
0.6	14.88

*Malik, M. R., "Prediction and Control of Transition in Supersonic and Hypersonic Boundary Layers," AIAA Journal, vol. 27, no. 11, November 1989, pp. 1487-1493.

Computational Results

- **Transition occurs at N = ~9.2**
- **Significant transition delay vs. smooth cone for CO2**
- **Air and N2 injection both *promote* transition**
- **Mass flux = 2.5 grams/sec (but over entire surface; "Malik cone")**
- **Smooth cone, x_{tr} = 63 cm**

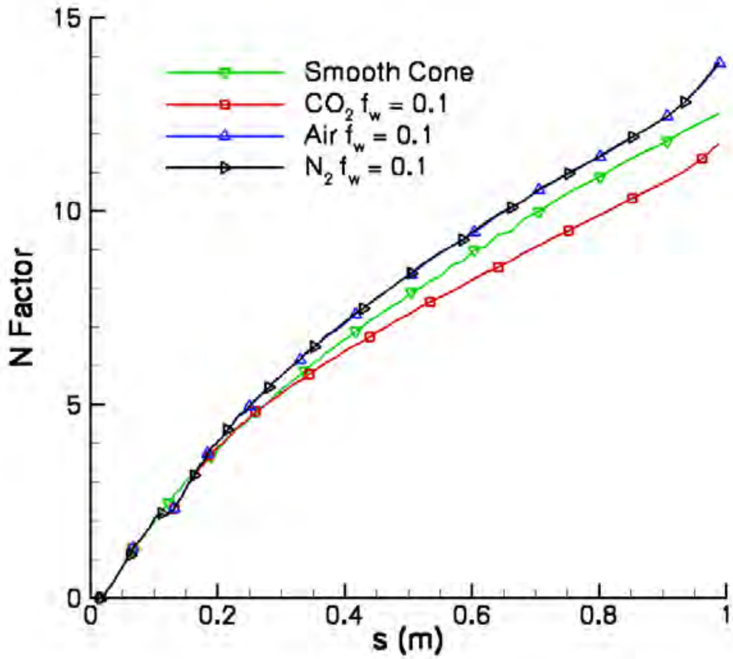

N factor versus distance along cone surface

From Wagnild et al 2010

Computational Results

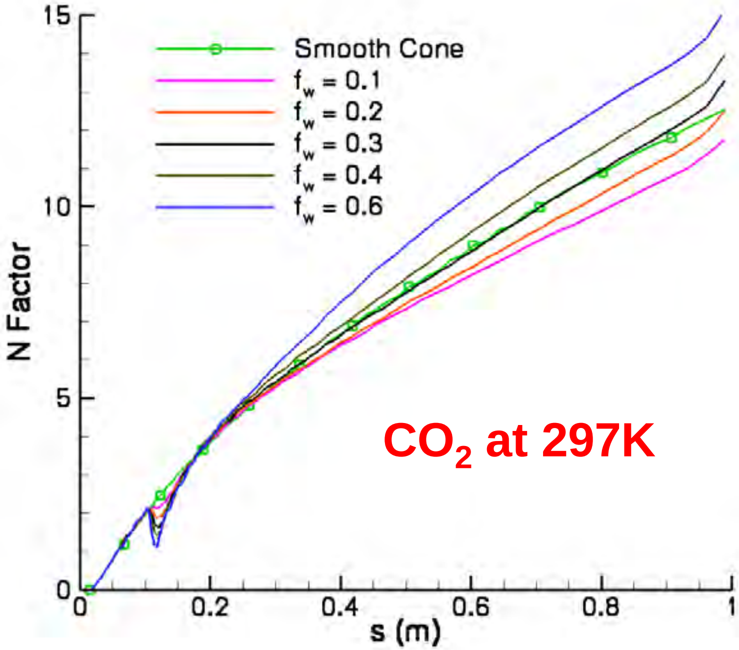

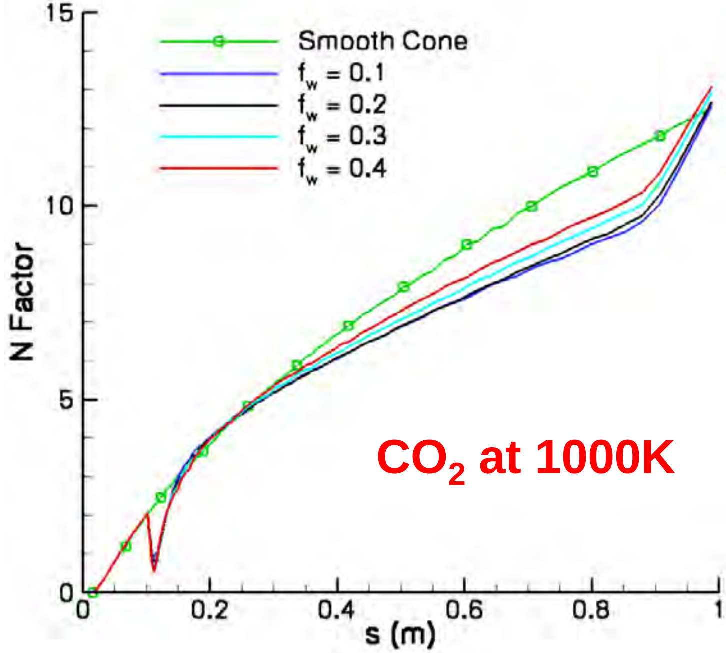

- **Transition delay predicted**
  - **Increase in CO_2 initially results in further delay but further increase causes more amplification**
- **For N_{cr} = 9.2**
  - **Smooth cone, x_{tr} = 63 cm, f_w = 0.1, x_{tr} = 72 cm**

- **Pre-heating further delays transition**
  - **CO_2 able to absorb acoustic energy earlier**
  - **Higher temperature gas could also contribute**
- **For N_{cr} = 9.2**
  - **Smooth cone, x_{tr} = 63 cm**
  - **f_w = 0.1, x_{tr} = 83 cm**

From Wagnild et al 2010

Effect of gas and Temperature on Transition Delay: CFD predictions

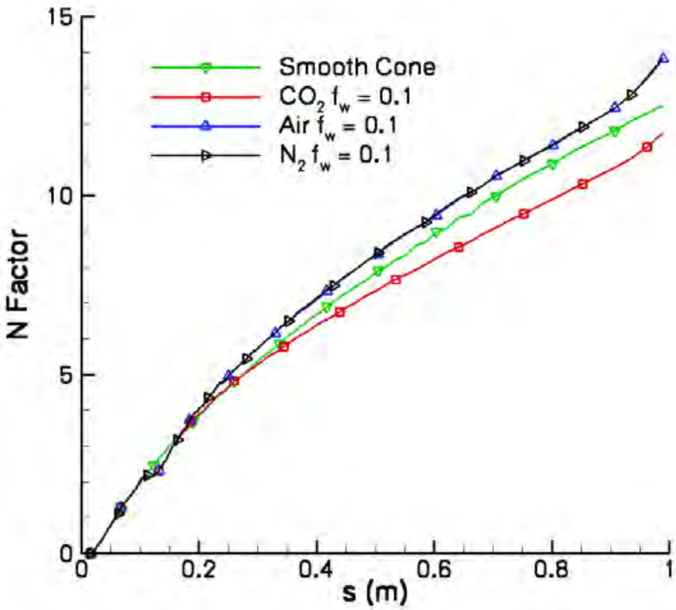

Alternate gases only increase disturbance

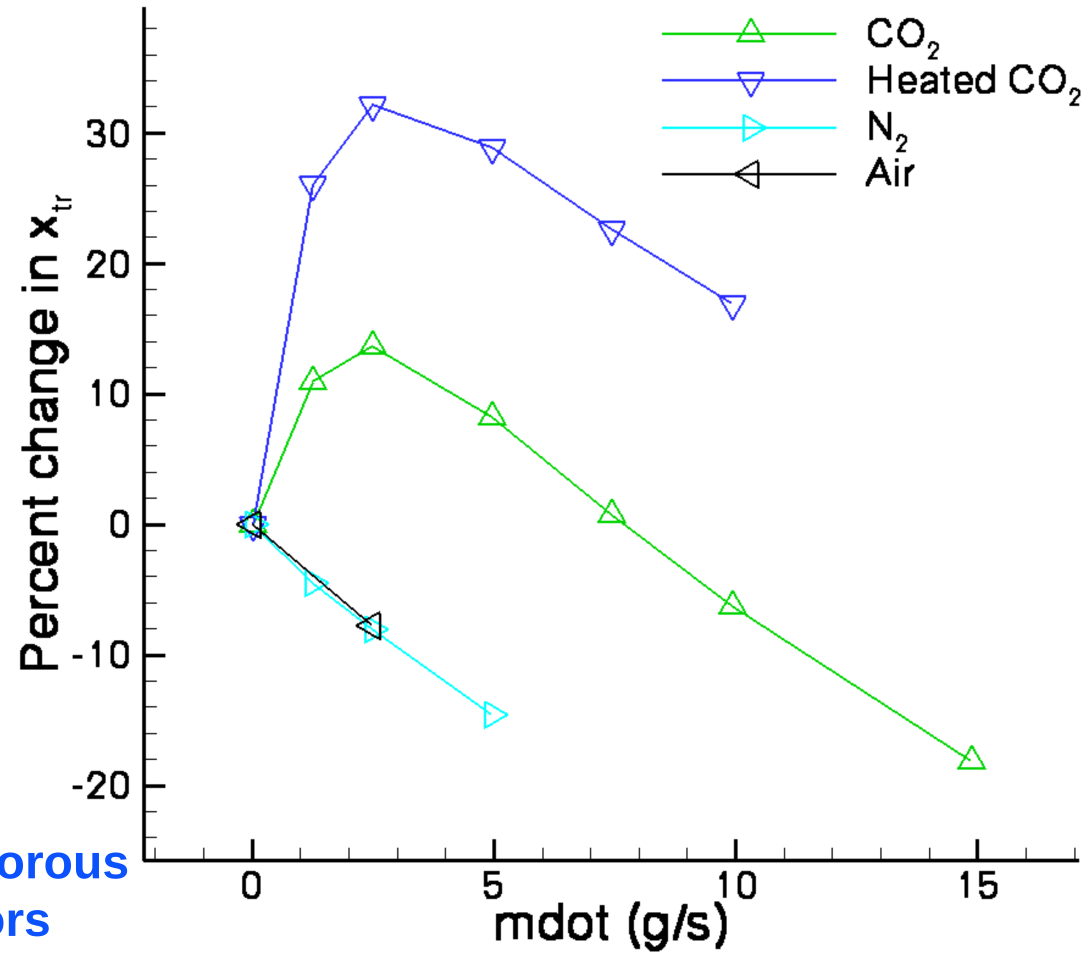

CFD predicts that for the current porous design and longer porous injectors transition could be delayed for optimum flow rates and temperature of CO_2

Citations

- **Aerospace America 2009 – Year in Review: Fluid Mechanics**

  "AFRL, Caltech, and the University of Minnesota have collaborated in a numerical and experimental study on control of high-speed boundary layers. The team has demonstrated significant delays in transition"

- **Annual Reviews of Fluid Mechanics 2011, 43:79-95. – Federov, A. "Transition and Stability of High-Speed Boundary Layers":**

"..Another way to stabilize the second mode and thereby delay transition is to add CO2 into high enthalpy boundary-layer flow (Leyva et al. 2009). The motivation for this new technique lies in the following findings: Molecular vibration and dissociation suppress the acoustic instability, and at relevant conditions for hypersonic flight, CO2 absorbs energy most strongly in the frequency band associated with the second mode.

The experiments of Leyva et al. (2009) on a sharp slender cone in the GALCIT T5 tunnel showed that the CO2/N2 free-stream blends (without injection) lead to significant delay of transition. The transition Reynolds number more than doubled for mixtures with 40% CO2 mole fraction compared with the case of 100% N2. A similar effect was noted in experiments using mixtures of air and CO2 as the test gas. Experimental and numerical studies of the CO2 injection system suitable for this LFC concept are in progress. The effect of the injection and the transition location is gauged by solving the PSEs and using the semiempirical *eN method (Wagnild et al.* 2010).."

Half-Porous/Half-Smooth Injector

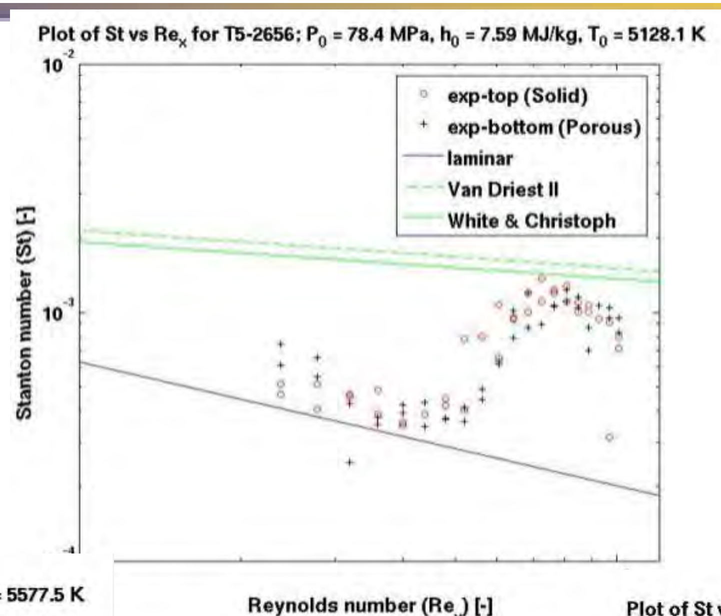

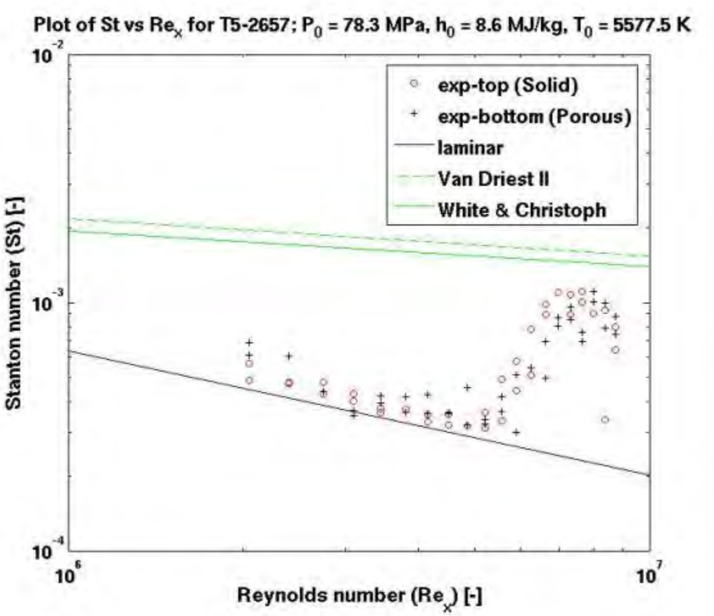

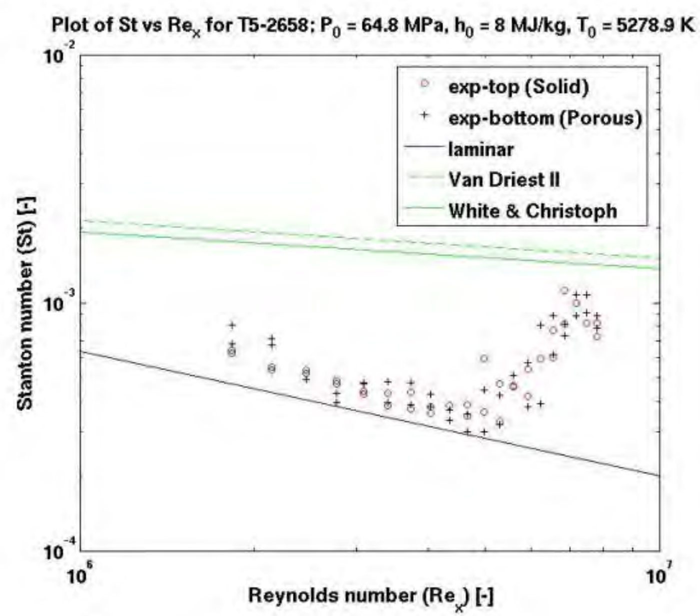

Boundary Layer Temperatures

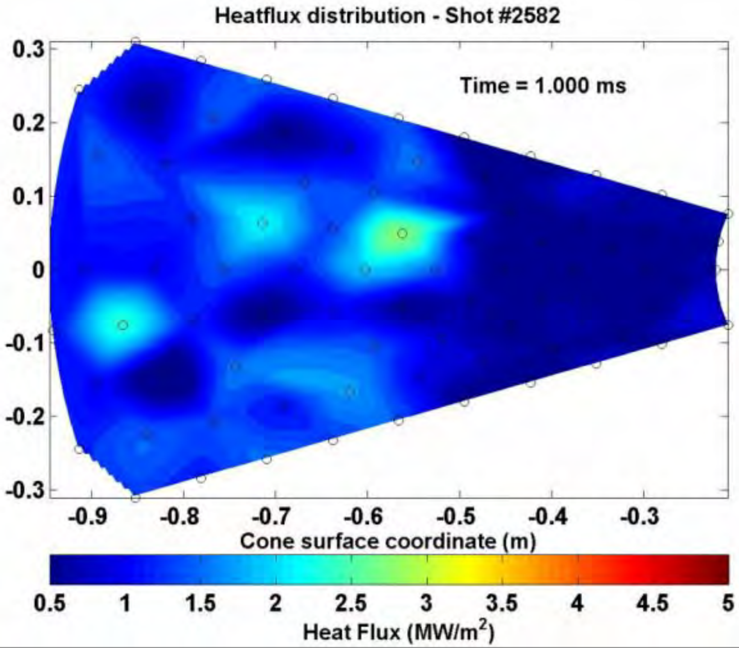

H_0 (MJ/kg)	P_0 (MPa)	T* (Eckert)	T_{edge}
5.69 – 5.92	~ 30	1465 K	779 K
8.29	53.8	2149 K	1272 K
8.60	**78.3**	**2246 K**	**1355 K**
8.85	53.2	2295 K	1395 K
9.46 – 10.32	~55	2725 K	1728 K

Latest →

Ongoing Challenges

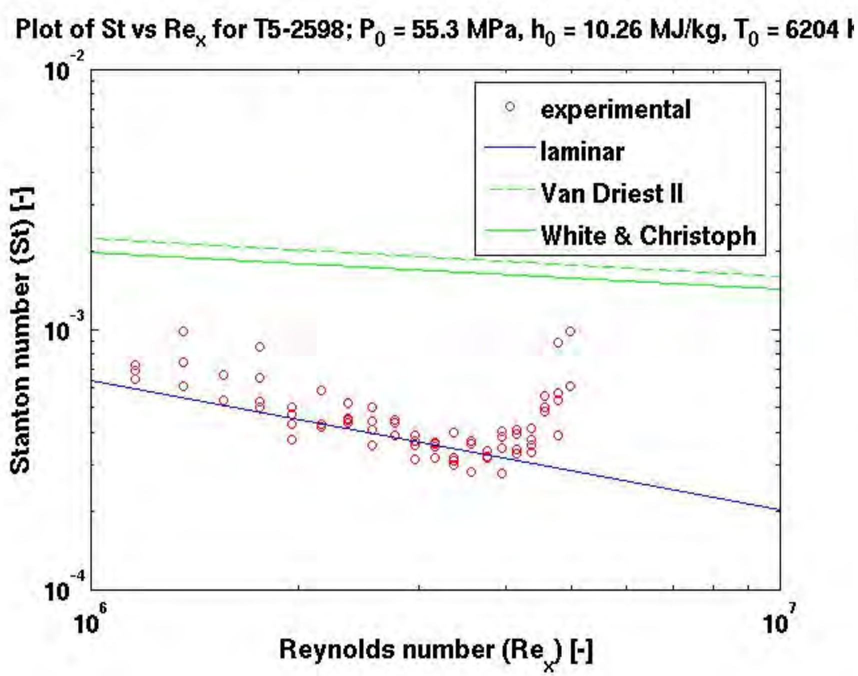

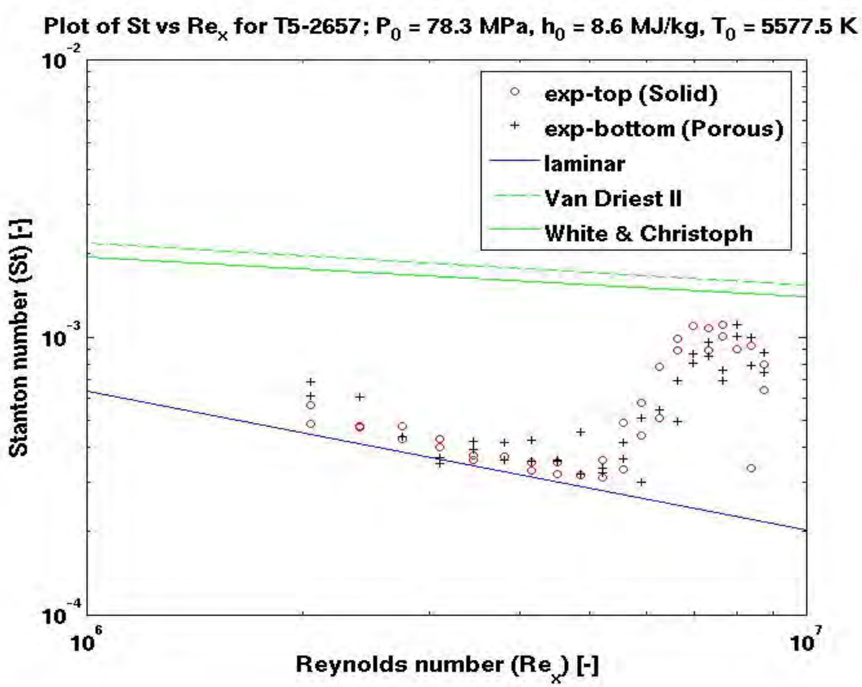

10.3 MJ/kg, 55 MPa
Natural transition @ 72 cm
Delay observed

8.6 MJ/kg, 78 MPa
Natural transition @ 54 cm
Delay NOT observed

- **In both cases, T* and T_e are above the critical 960K for CO_2**
- **Why is delay not observed for injection in the case on the right?**

Ongoing Challenges

Possible Explanation

- N-factor at transition is similar (5.0-5.6 for a noisy tunnel) in both cases
- N-factor at the injector section location (13.3 cm from the tip) is therefore significantly higher for the case with earlier natural transition (right hand plot on previous slide)
- To suppress the 2nd mode, mixing must be achieved at a relatively low (but not precisely known) N-factor

Variables to optimize for attaining delay by injecting CO_2

- N-factor at injection location
- (T^* or T_e of boundary layer base flow) / (T_{vib} of CO_2)
- (mixing distance for CO_2 with boundary layer base flow) / (cone length)
- (CO_2 mass flow rate) / (boundary layer base mass flow)

Collaboration with Alexander Fedorov – Moscow Inst of Physics and Tech

- Determine how low the N-factor at injection must be, and where this physically occurs on the cone
- Redesign of injector section to move it closer to the tip, achieving injection before the 2nd mode acoustic waves appear

Conclusions

- At 10 MJ/kg enthalpy, demonstrated delay versus Argon injection and also versus a smooth injector
  - CO_2 does make a difference!
- Selected a new condition at about 8-9 MJ/kg for further study
  - Meant to show a greater effect because natural transition occurs near the middle of the cone
  - However, CO_2 injection did NOT seem to delay transition at this condition
- Designed and installed a half-porous, half-smooth porous injector
  - Provides a non-injection "control" with every injection experiment
- Collaboration with Alexander Federov to for theoretical/computational input into injector design and placement

Questions ?

Back up

Preliminary results from resonantly enhanced field focused schlieren system (REFFSS)

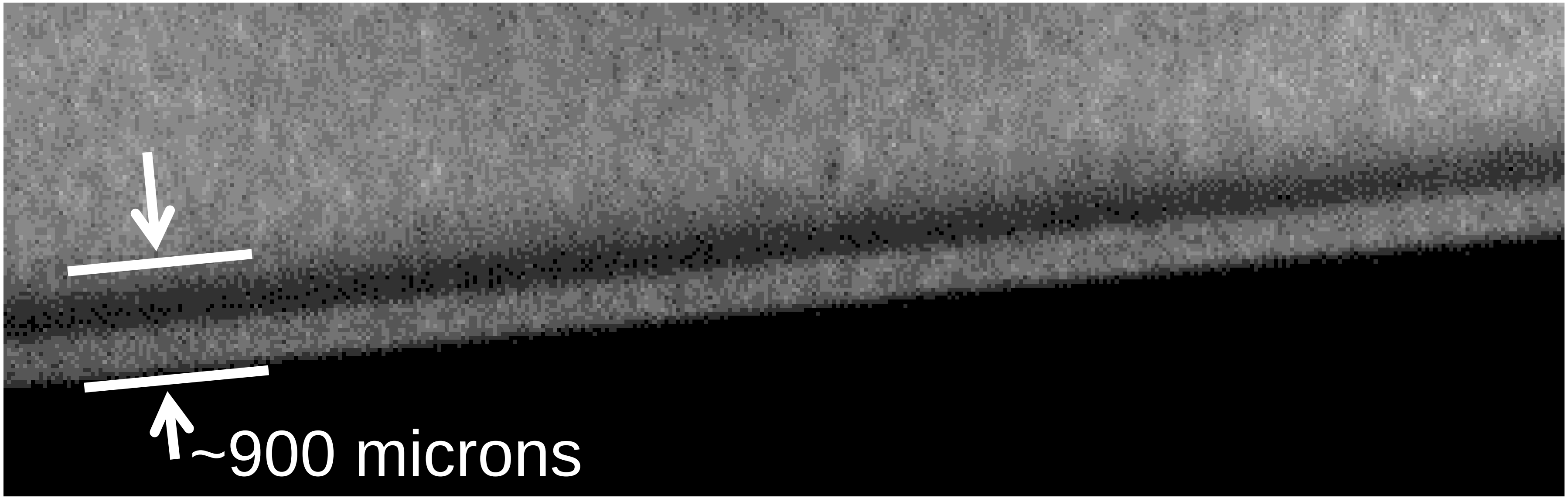

Preliminary results from resonantly enhanced field focused schlieren system (REFFSS)

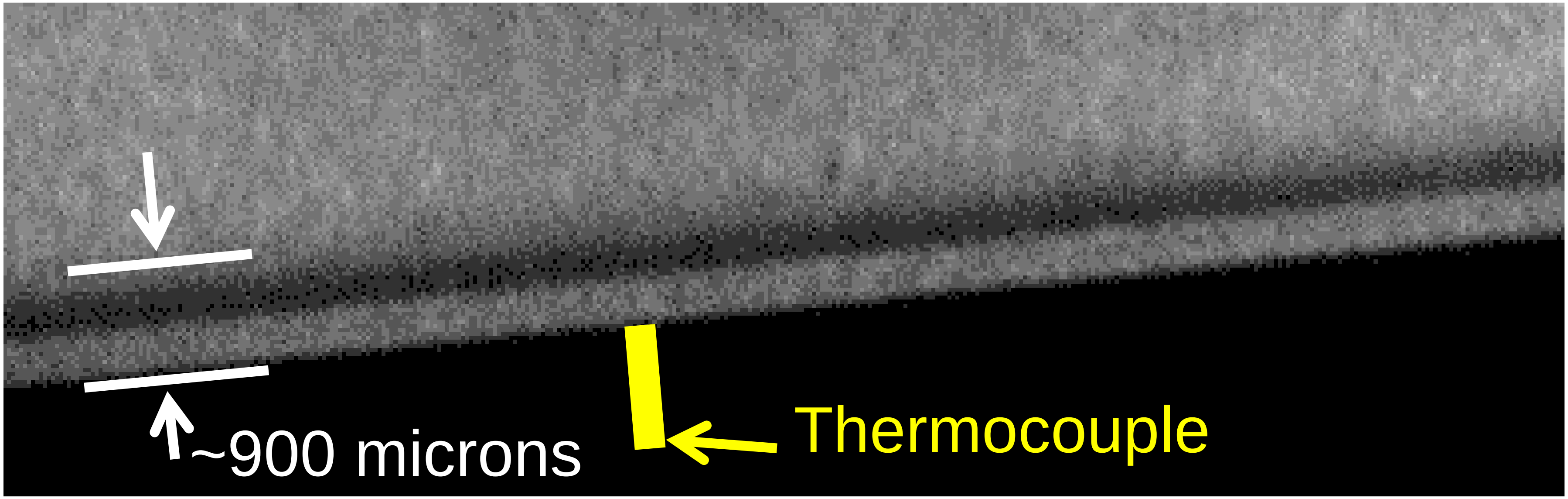

Preliminary results from resonantly enhanced field focused schlieren system (REFFSS)

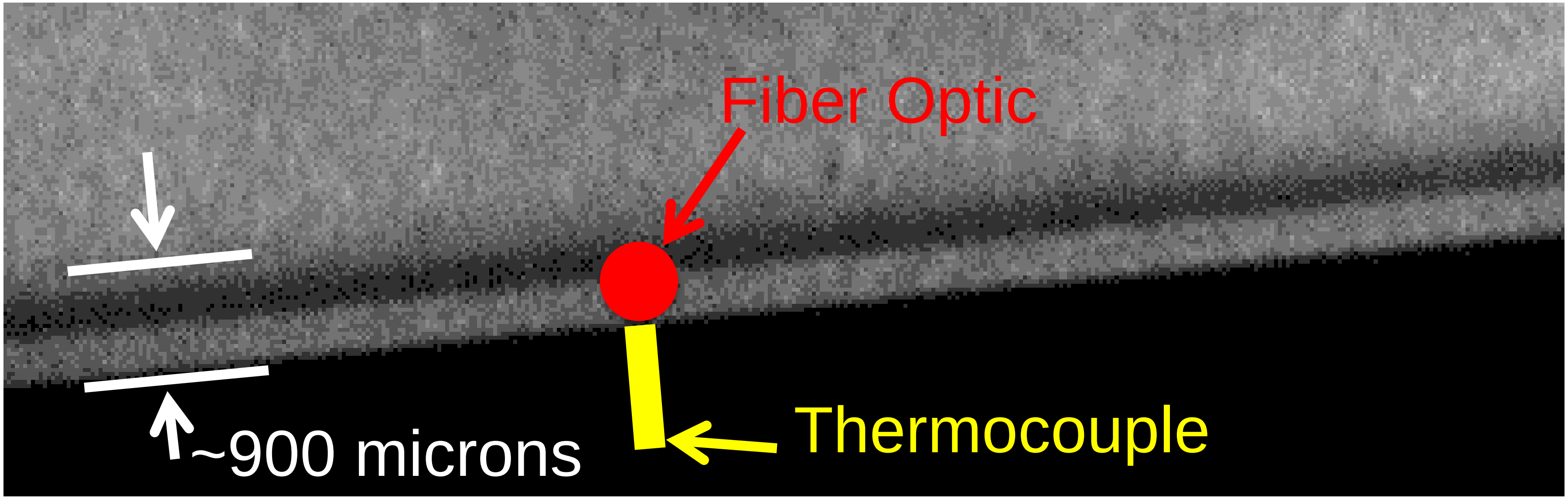

Distribution A: Approved for public release; distribution unlimited

Preliminary results from REFFSS

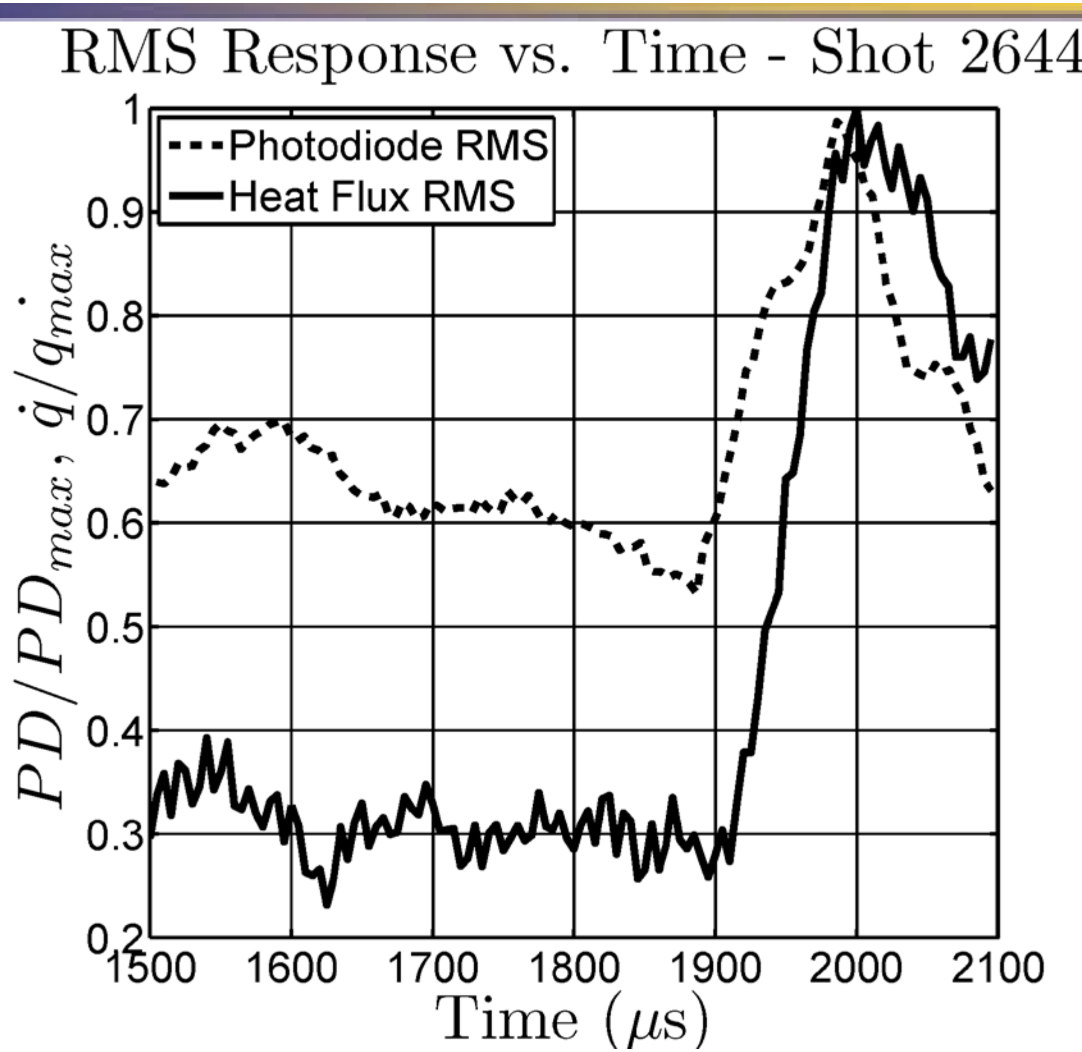

h_R = 6 MJ/kg ; p_R = 50 MPa

Preliminary results from REFFSS

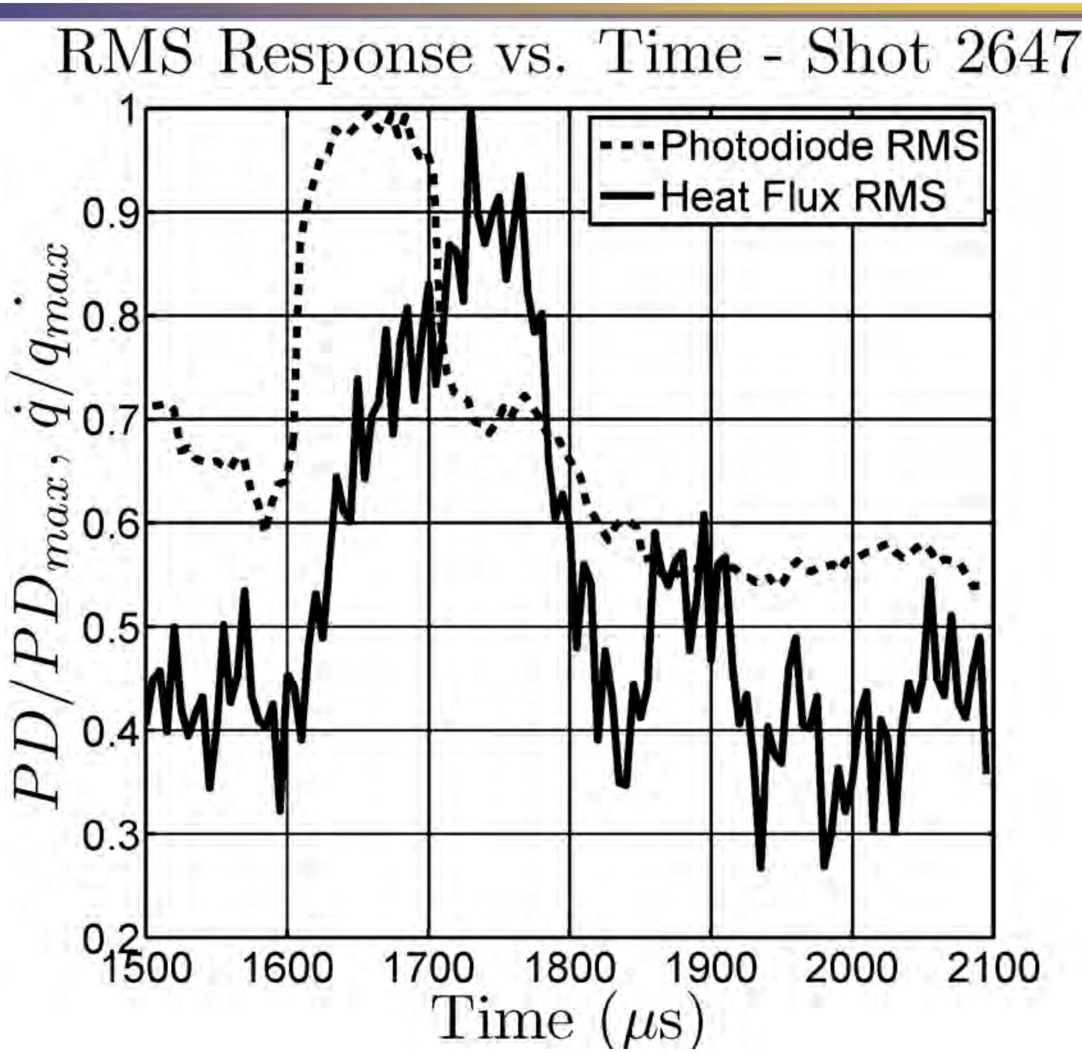

h_R = 6 MJ/kg ; p_R = 30 MPa

Heated Carbon Dioxide

- **Baseline condition similar to shot 2541**
  - **Test gas is air**
  - **Free-stream Mach is 5.3**
  - **Isothermal wall at 293 K**
- **Pre-heated CO_2**
  - **Momentum of injection matched with 13.5 g/s of cold carbon dioxide**
- **Increase in heating results in decreased amplification**
  - **Reduction in amplification more efficient near 1000 K**

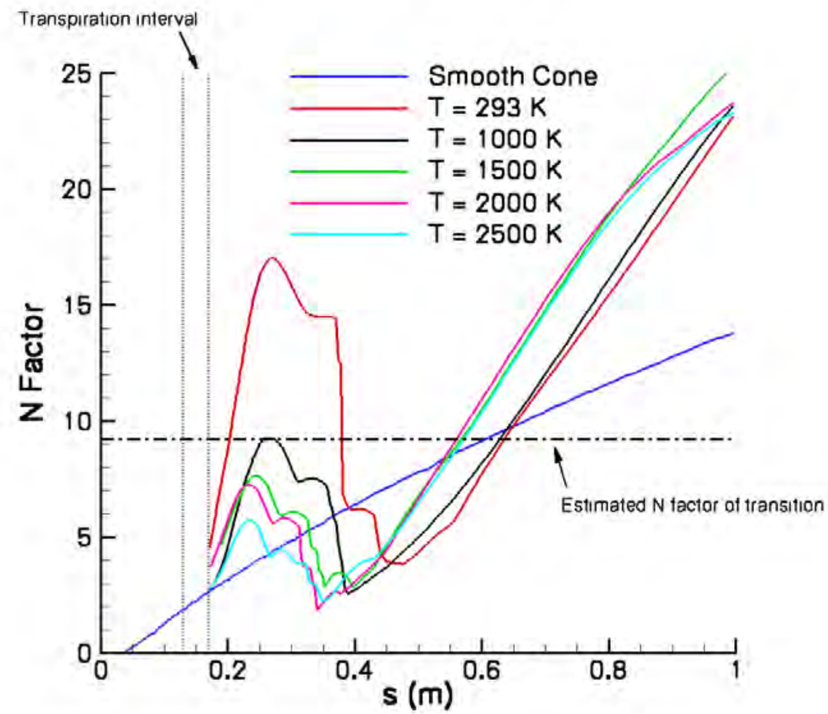

N factor versus distance along cone surface

Stagnation Conditions		Free-stream Conditions	
Pressure (MPa)	50.92	Density (kg/m^3)	0.05572
Temperature (K)	5968.5	Temperature (K)	1369.4
Entalpy (MJ/kg)	9.51	Velocity (m/s)	3957.9

Computational Model

- Computations done using STABL software suite
  - Mean flow
    - 2nd order accurate fluxes
    - Modified Steger-Warming
    - 1st order Implicit DPLR method for time integration
    - Finite rate chemistry and T-V energy exchange
  - Disturbances
    - STABL PSE-chem solves the parabolized stability equations
    - PSE predict amplification of disturbances
    - Finite rate chemistry and T-V energy exchange
    - Semi-empirical e^N method used for determining transition location

Transition Determination Uncertainty

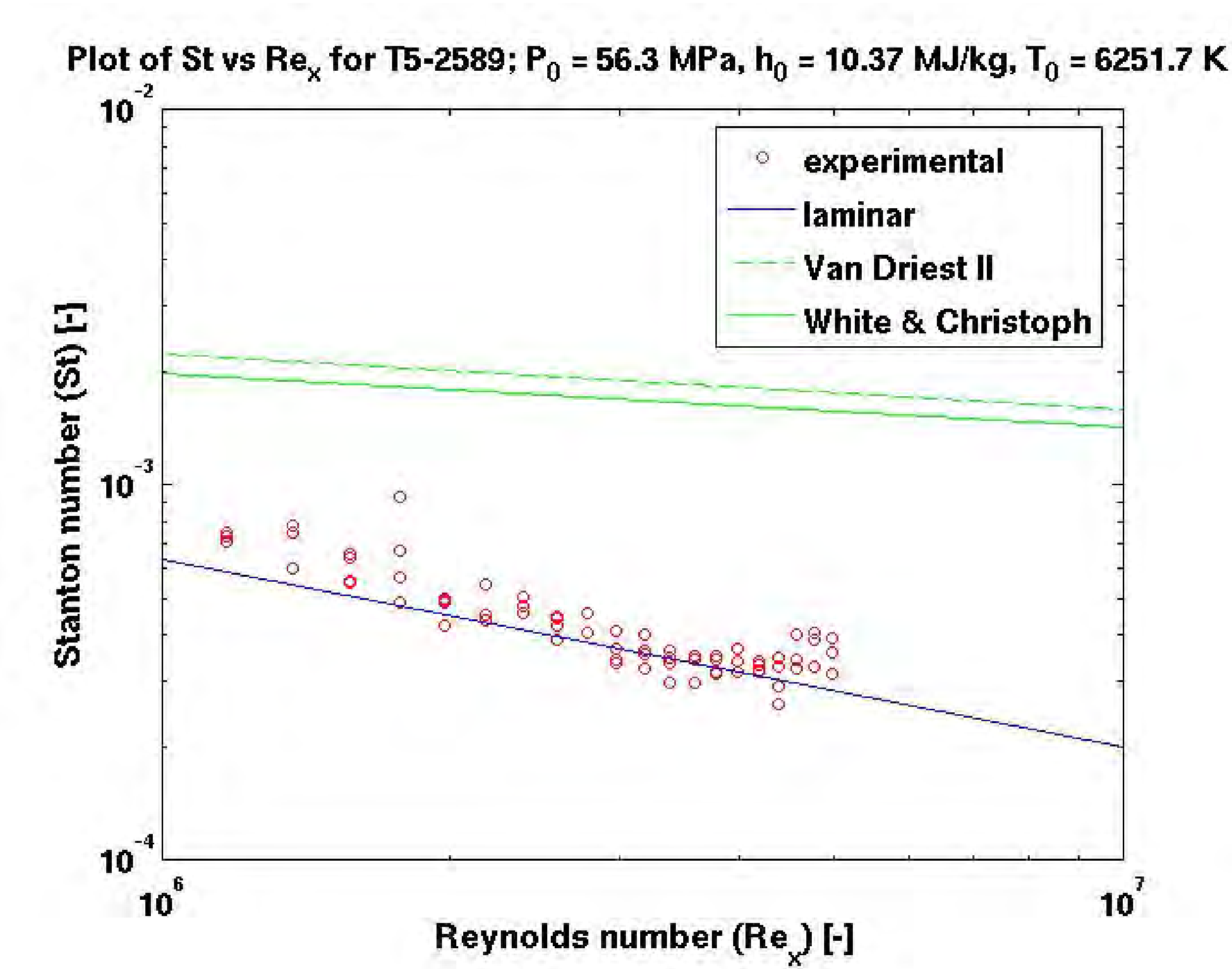

Porous Injector Results: Intermittency Method

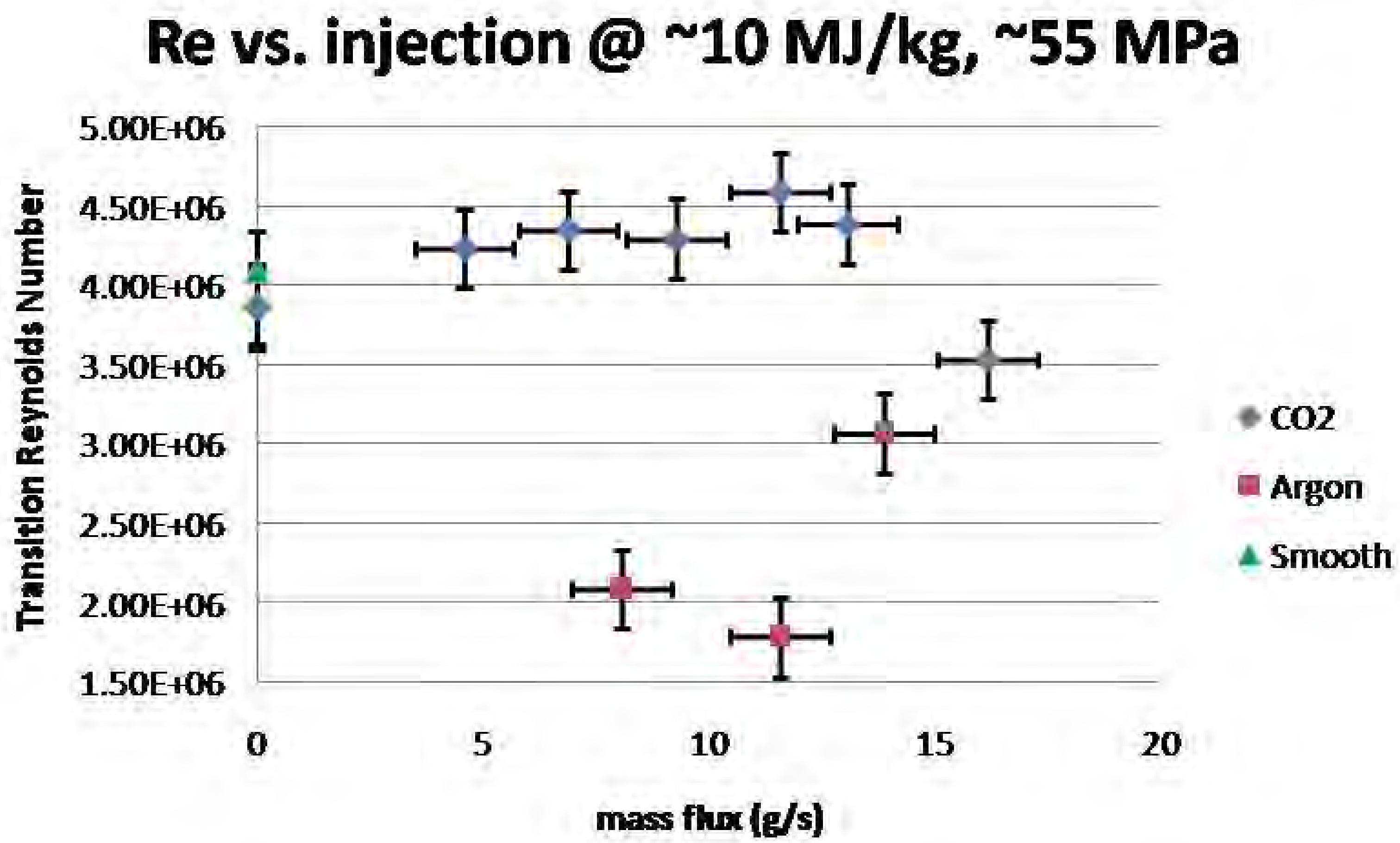

Data Reduction: Intermittency Method

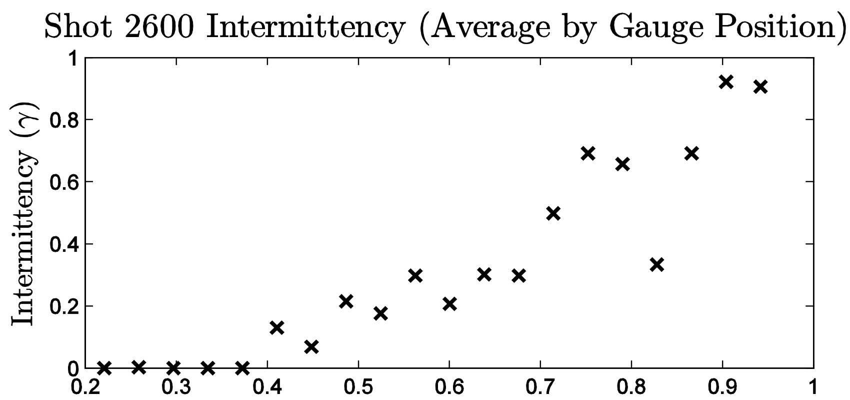

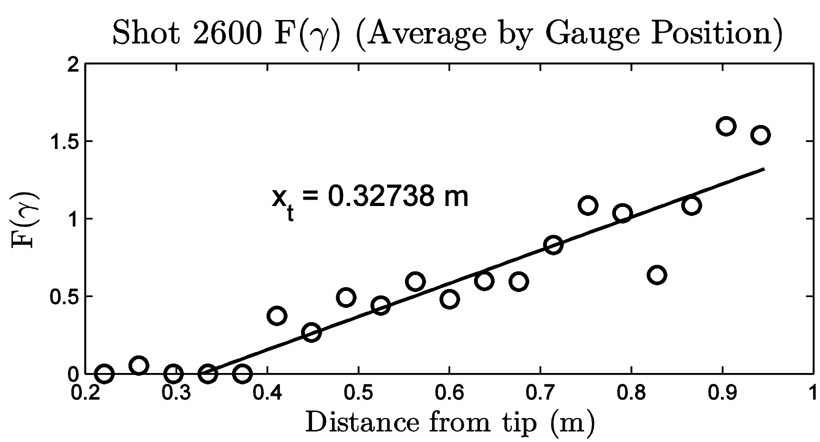

Turbulent intermittency

Transition location determined from intersection

Data Reduction: Intermittency Method

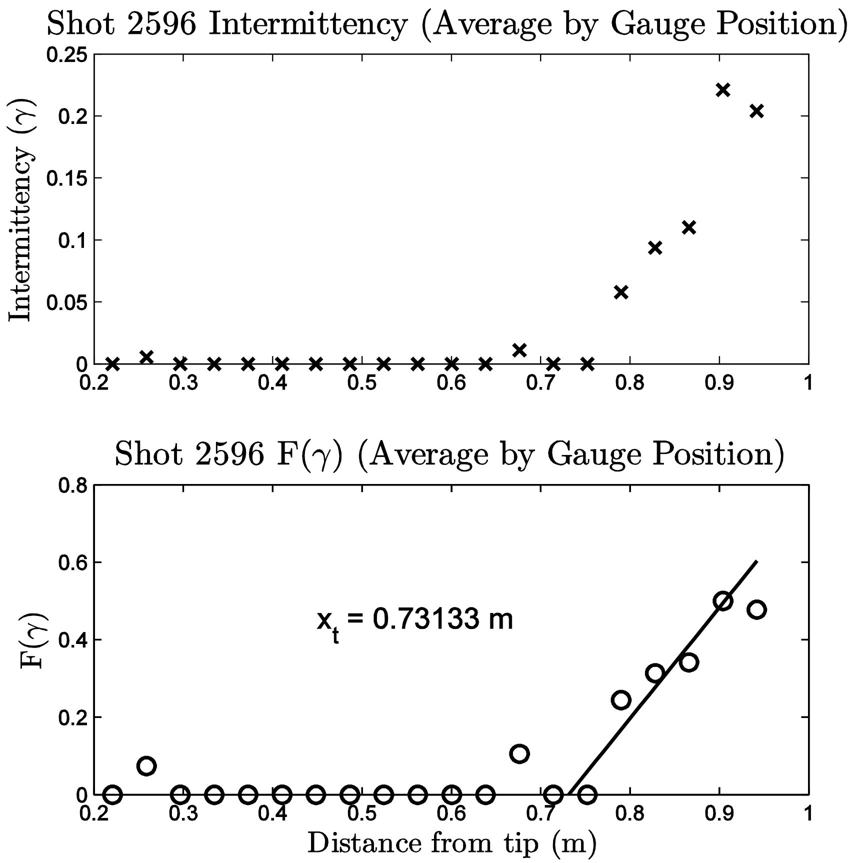

Turbulent intermittency

Transition location determined from intersection

Porous Injector Results (10 MJ/kg)

10-micron Porous Injector (**Ar** injection at 11.6 grams/sec)

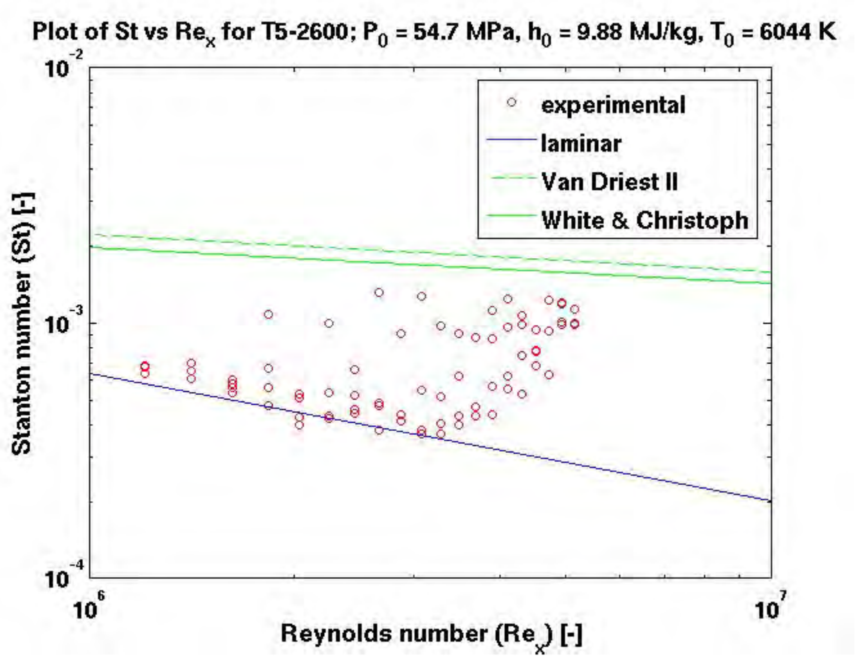

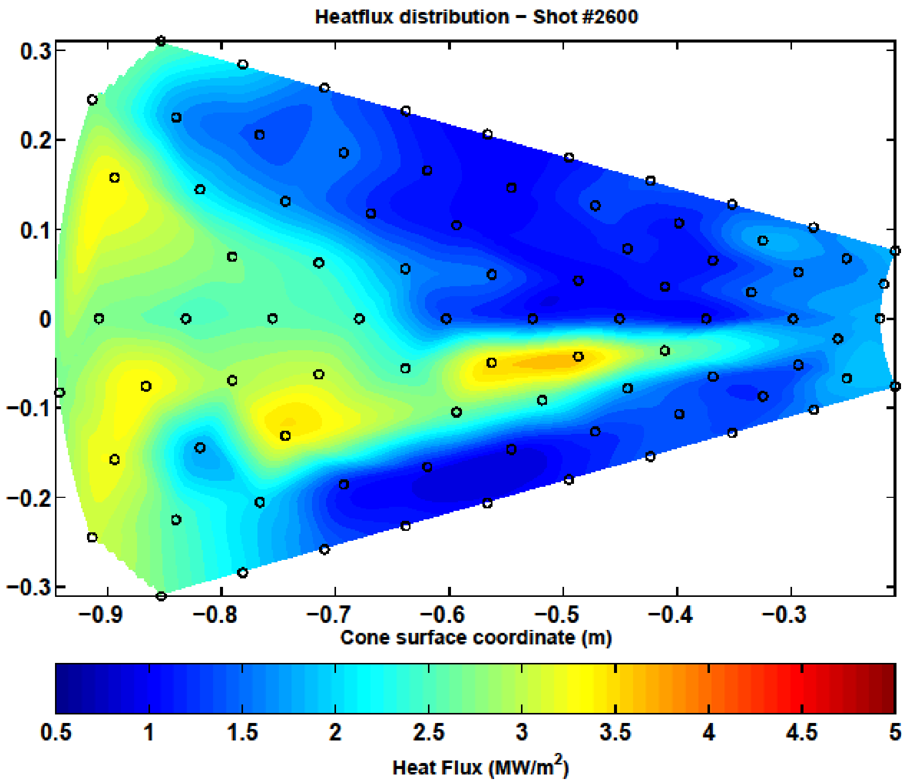

Transitional flow

Re_{tr} = 2.88 x 10^6

Porous Injector Results (10 MJ/kg)

10-micron Porous Injector (no injection)

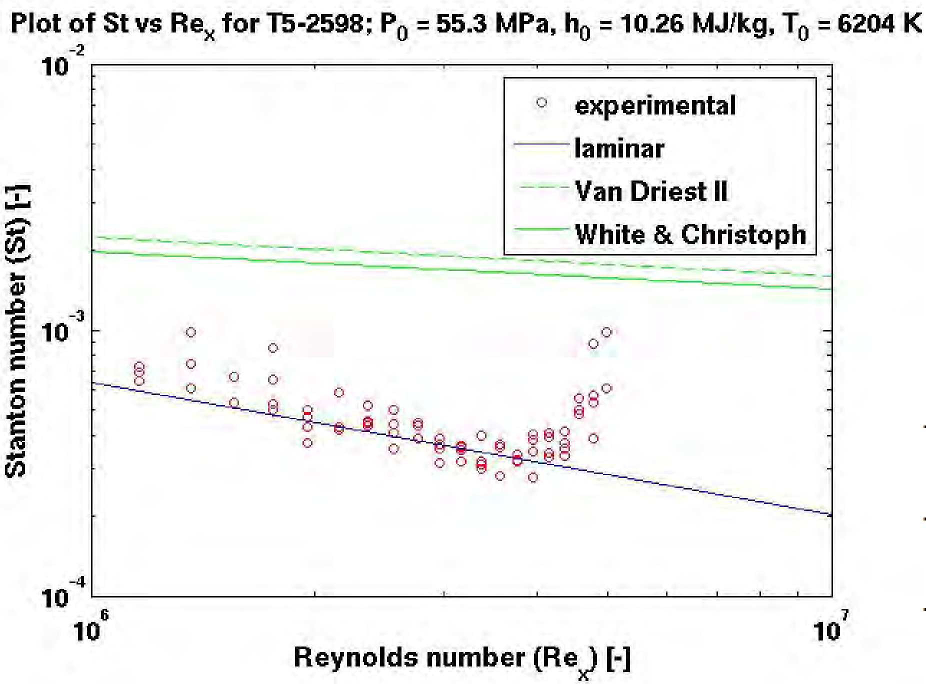

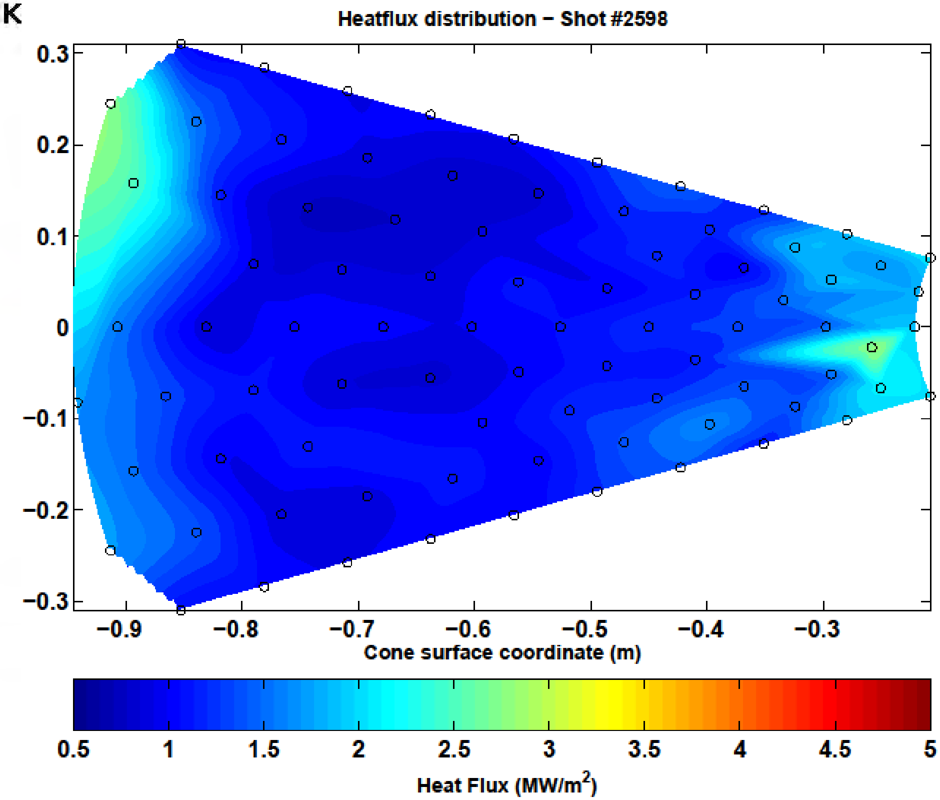

Initially laminar flow

Re_{tr} = 4.12 x 10^6

Porous Injector Results (10 MJ/kg)

10-micron Porous Injector (**CO_2** injection at 11.6 grams/sec)

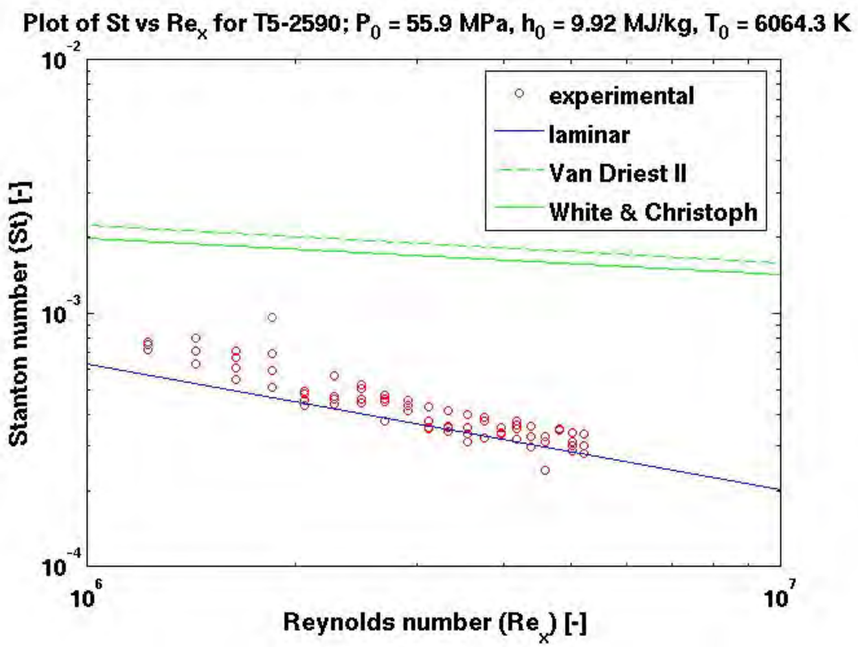

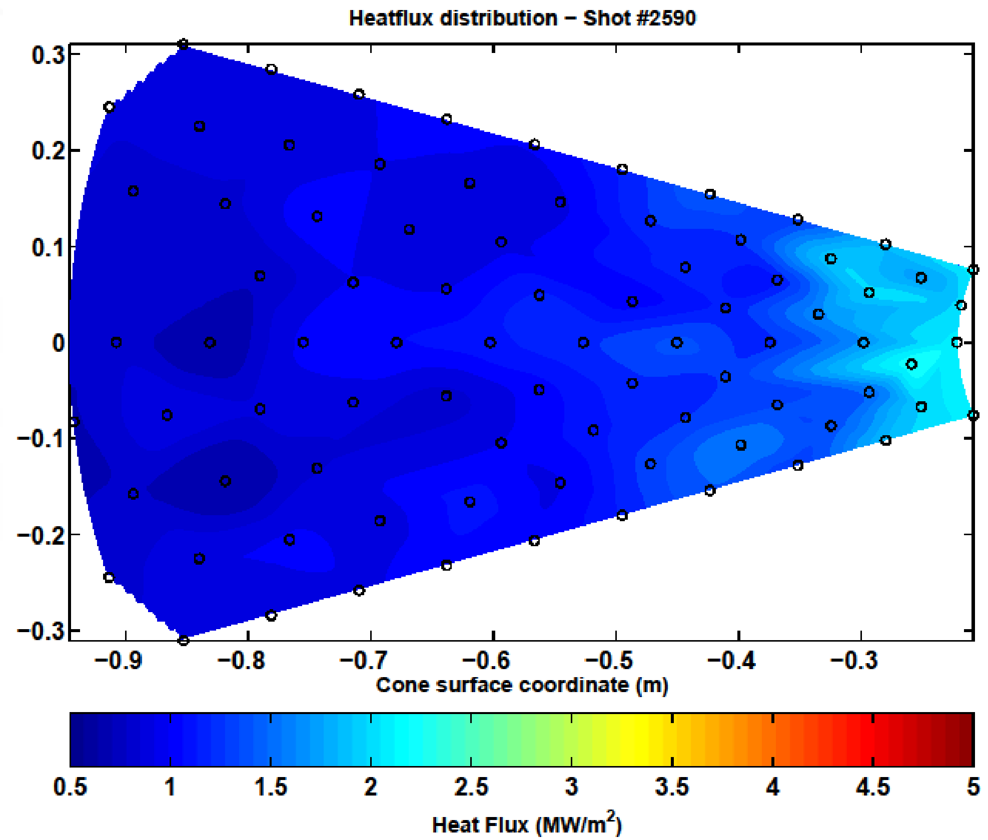

Completely laminar flow

$Re_{tr} >= 5.22 \times 10^6$

Porous Injector Results (10 MJ/kg)

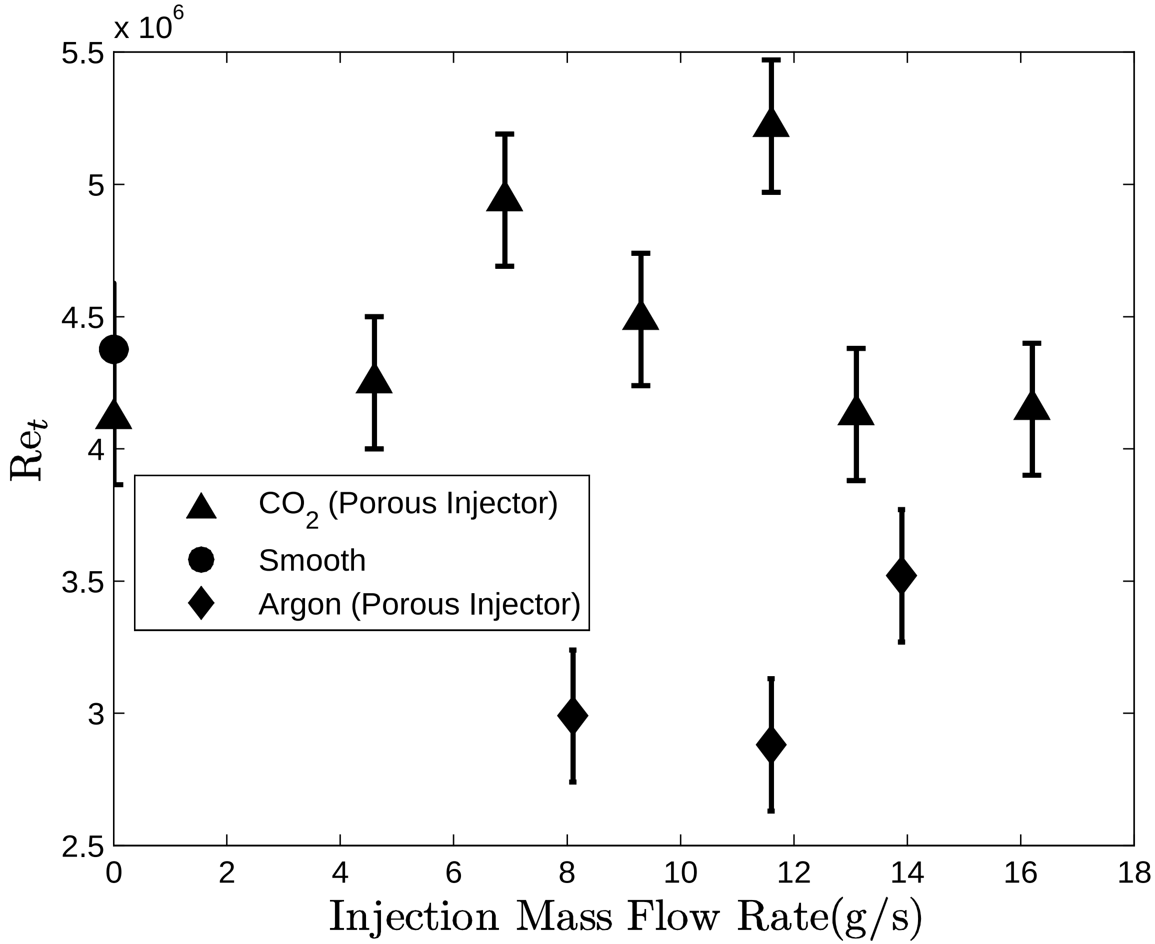

Summary of results (average heat transfer method)

Porous Injector Results (10 MJ/kg)

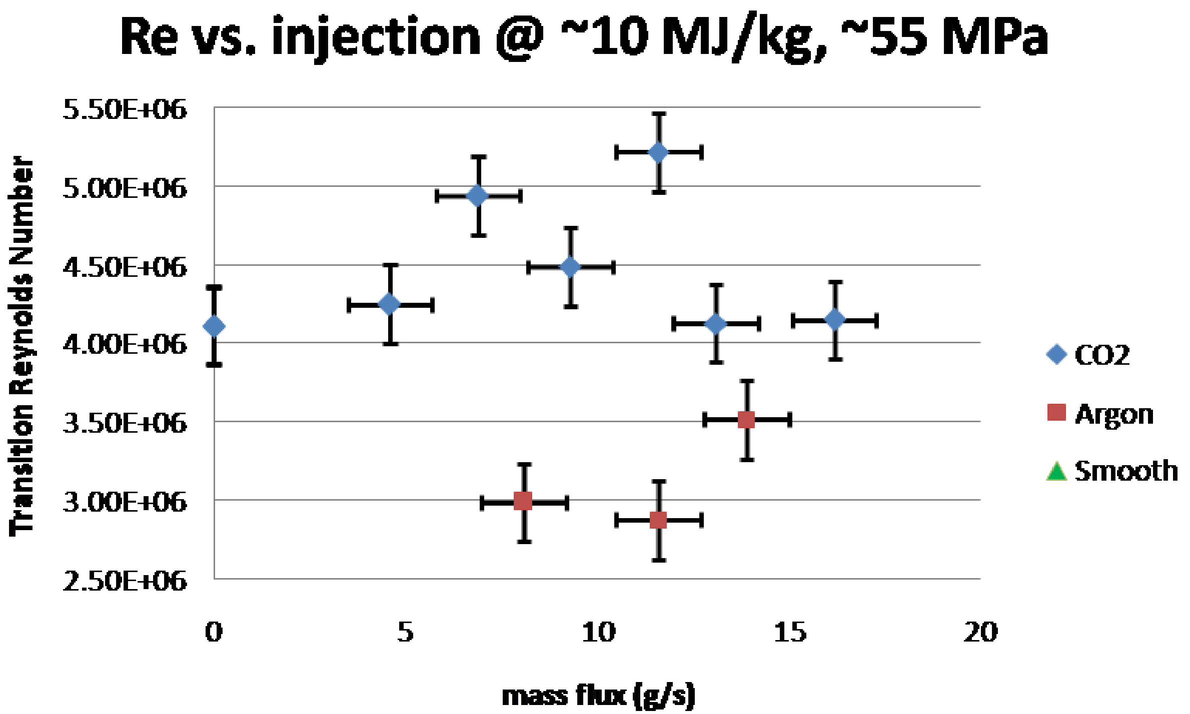

Two porous control shots

Porous Injector Results (10 MJ/kg)

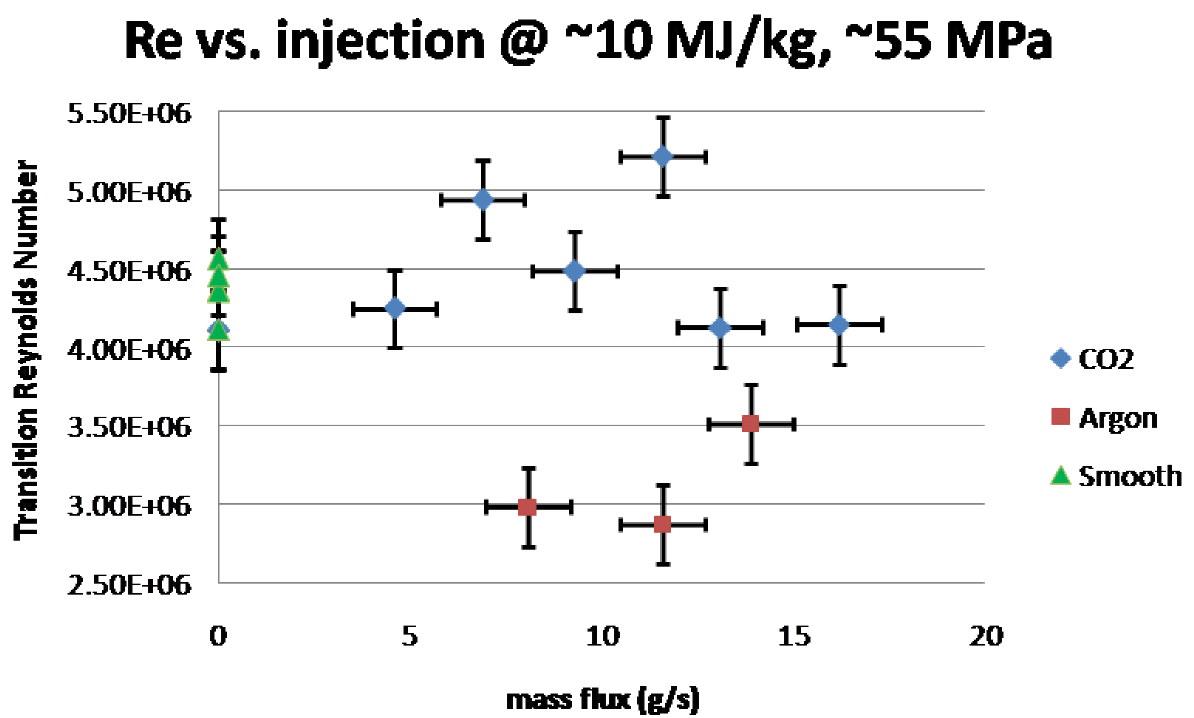

Five smooth control shots

Porous Injector Results (6 MJ/kg)

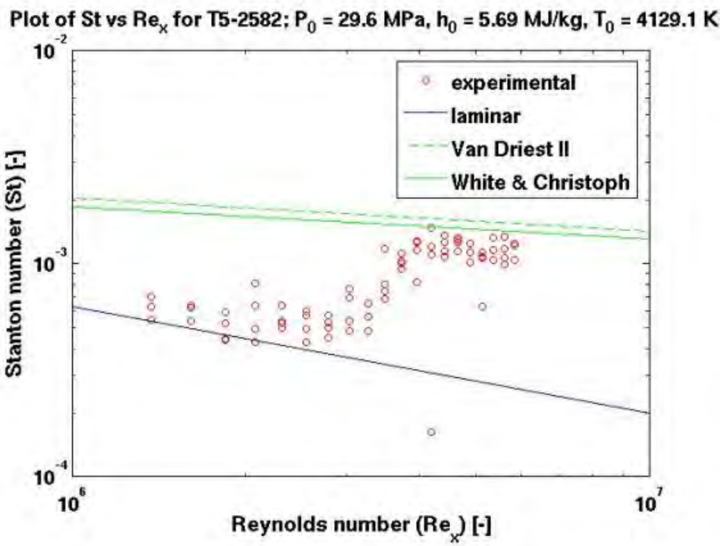

Porous tip – no injection vacuum plenum

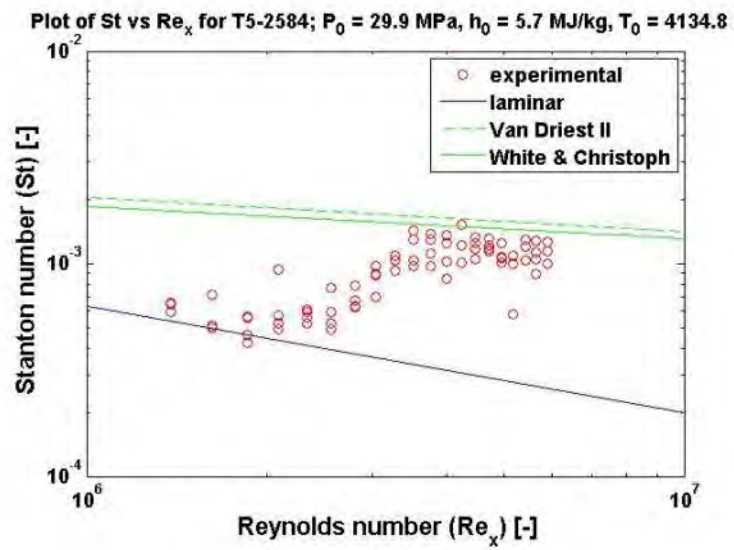

CO_2 injection 4 g/s

Ar injection 4 g/s

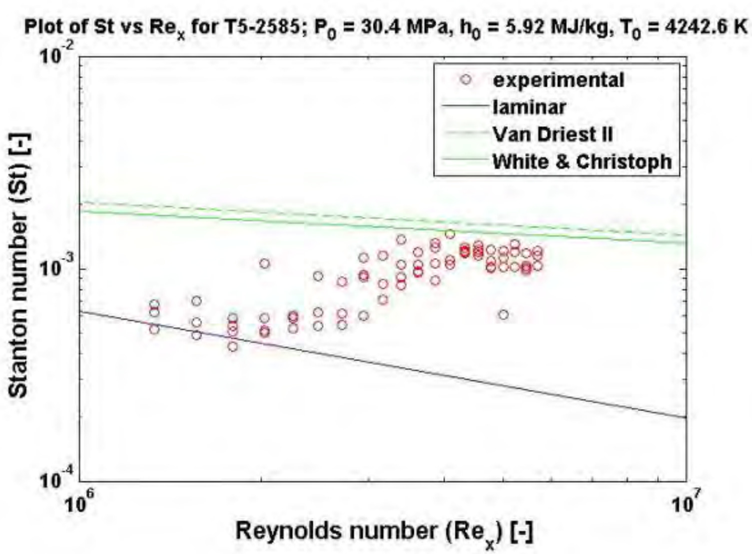

Injection of CO_2 and argon destabilize boundary layer and transition occurs earlier at lower enthalpy/temp.

Qualitative visualization

Before shot

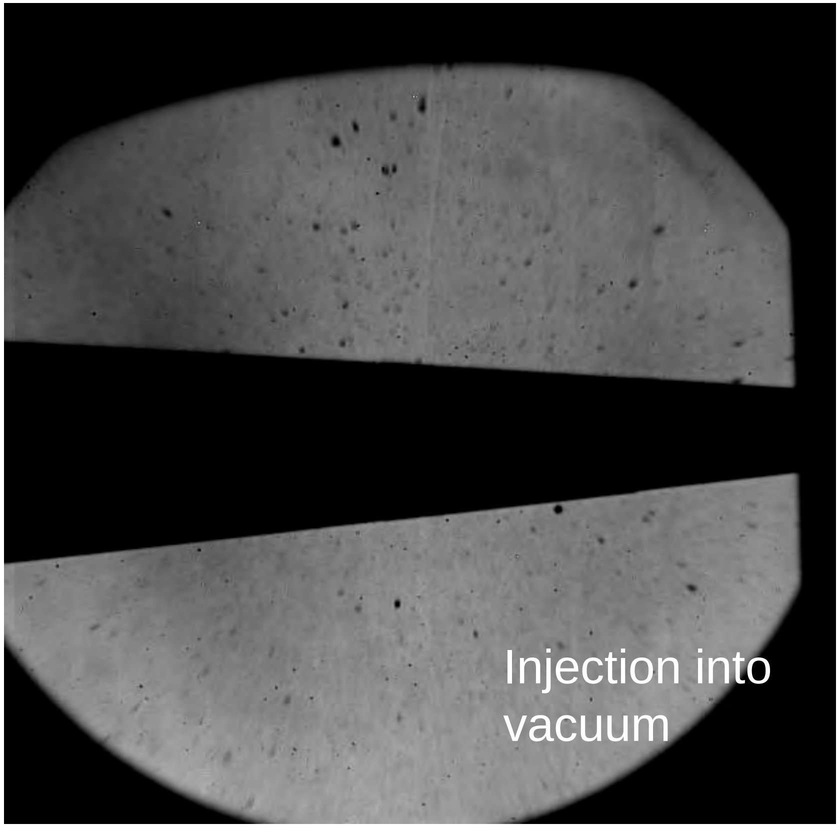

Porous Injector with cone downstream and 80 psi injection

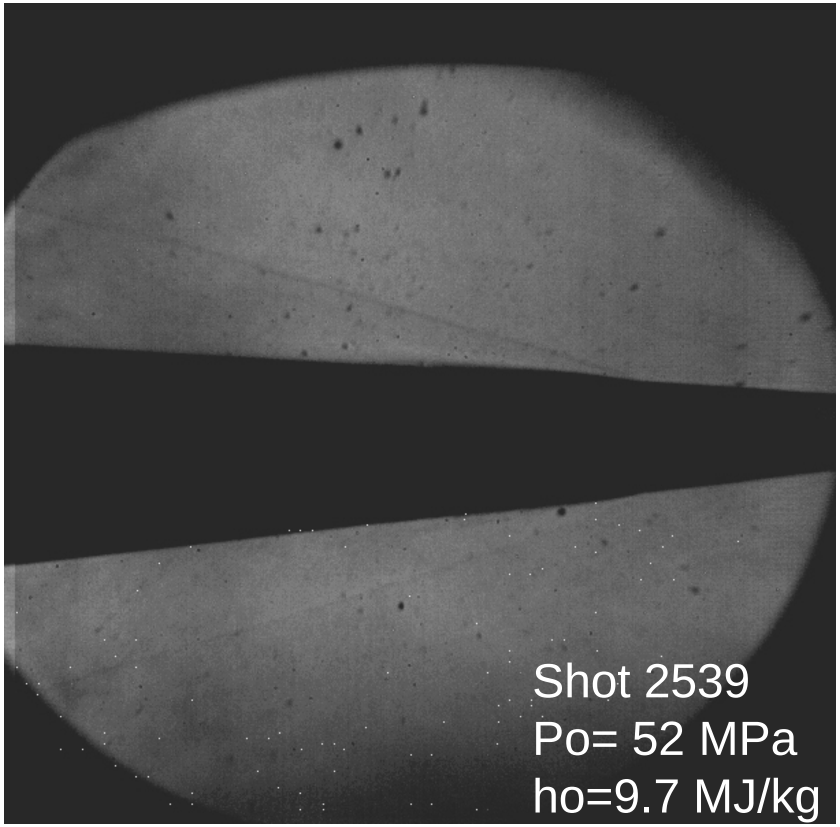

Schlieren seems to capture the CO2 injection clearly

Porous Injector Results

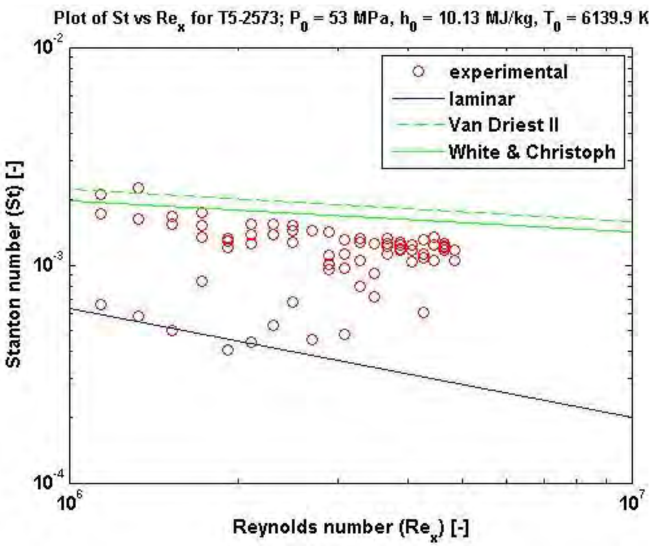

CO_2 injection
at 18.5 g/s

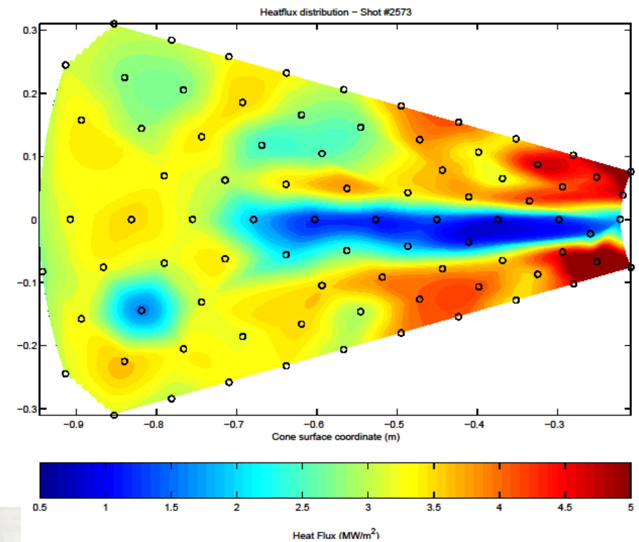

Immediately turbulent flow (streak due to injector flaw)

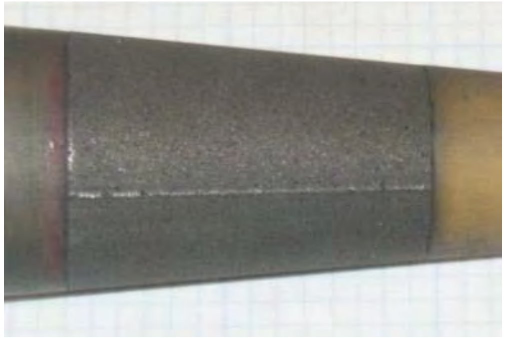

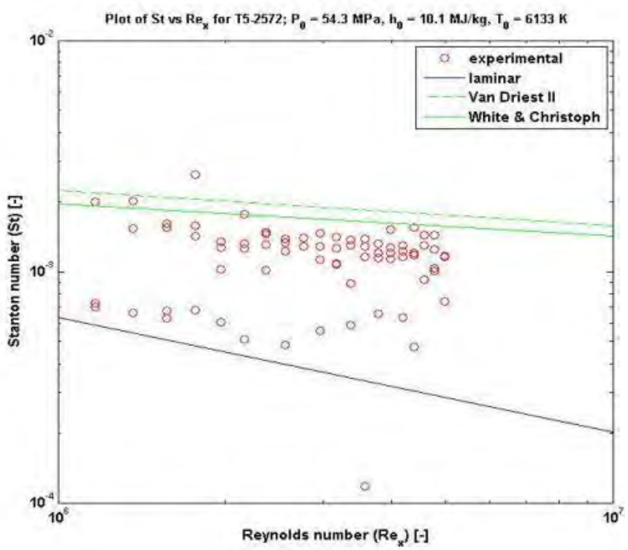

CO_2 injection
at 26.6 g/s

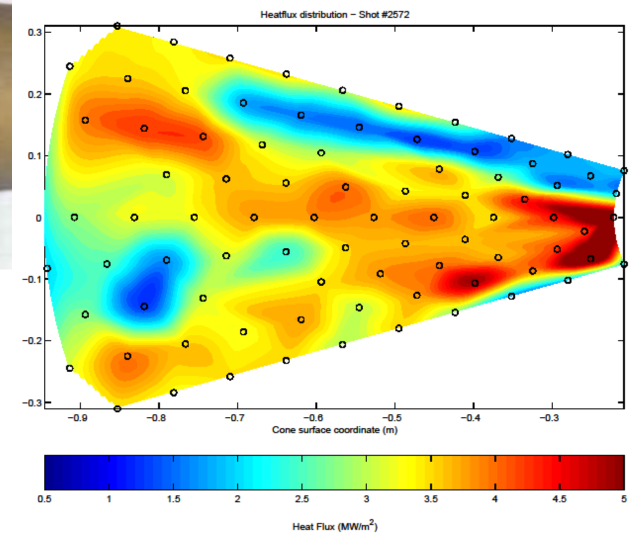

CFD test conditions

Gas Composition (by mass fraction)	
N2	0.7345
O2	0.1844
NO	0.0654
N	0.0
O	0.0157

Why vibration relaxation and dissociation damp acoustic waves

- **Theory known for decades (Lighthill, 1956, Herzfeld and Litovitz, 1959, Clarke and McChesney, 1964, Vincentti and Kruger 1967)**
- **Following Clarke and McChesney, the linearization of perturbations of the N-S equations leads to damping curve as shown – Maximum damping occurs when $\omega\tau = a_{f/}a_e$**
- **Relaxation processes such as molecular vibration and dissociation cause damping of acoustic waves through** ***phase lag between pressure and density***

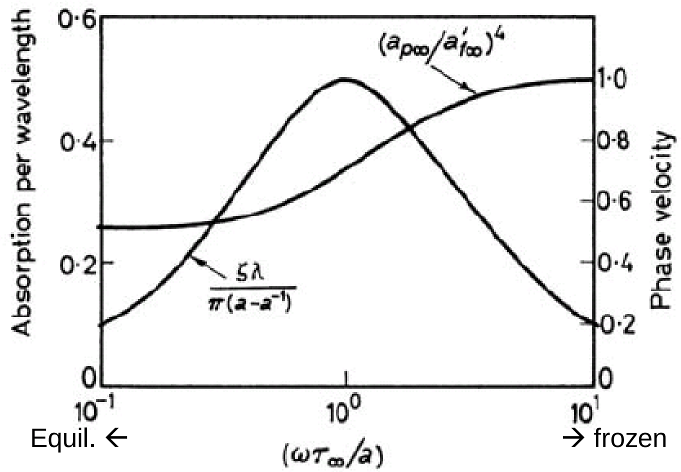

From Clarke and McChesney

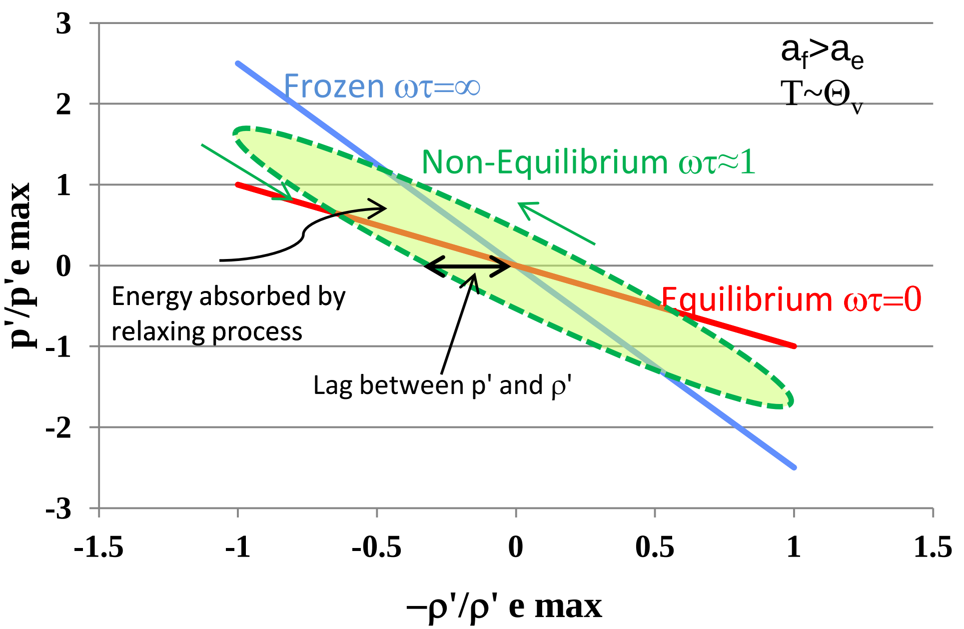

First injector models

Model No.	Hole diameter, d (mm)	No. Rows	Injection angle, α (deg)
1	0.51	2	12
2	0.76	1	11
3	0.76	1	12
4	1.02	1	11

Injector Variants

Model No. 1

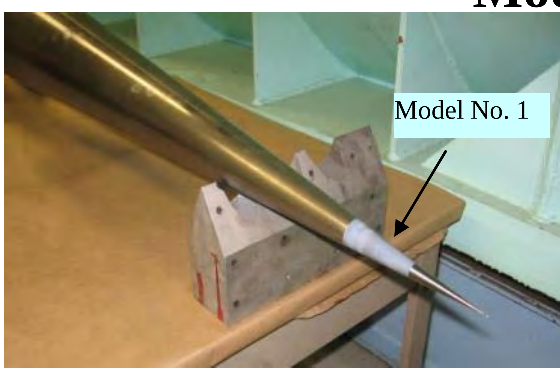

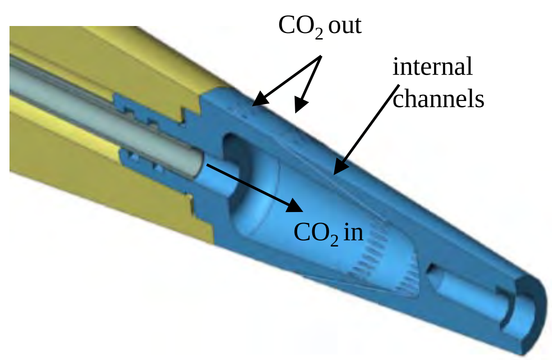

Model No. 2

Four injectors designed and built

Back-up charts

REFERENCES

1. Hornung, H.G., Adam, P.H., Germain, P., Fujii, K., Rasheed, A., “On transition and transition control in hypervelocity flows,” *Proceedings of the Ninth Asian Congress of Fluid Mechanics*
2. Fujii, K., Hornung, H.G., “Experimental investigation of high-enthalpy effects on attachment-line boundary layer transition,” *AIAA Journal, Vol. 41, No. 7, July 2003.*
3. Johnson, H.B., Seipp, T.G., Candler, G.V., “Numerical study of hypersonic reacting boundary layer transition on cones,” *Physics of Fluids, 10 (10): 2676-2685 Oct. 1998.*

Vibrational temperatures

species	M_w g/mol	$\sigma\Theta_{rot}$ K	h_f^o J/mol	g_v	Θ_v K	g_{e_o}	g_{e_i}	ϵ_e J/mol
N_2	28.016	5.79	0.0	1	3353.2	1	3	6.015×10^5
							6	7.136×10^5
							1	7.342×10^5
O_2	32.000	4.16	0.0	1	2239.0	3	2	9.225×10^4
							1	1.579×10^5
							3	4.320×10^5
							3	5.960×10^5
Ar	39.944	–	0.0	–	–	1	5	1.115×10^6
							3	1.122×10^6
N	14.008	–	4.713×10^5	–	–	4	6	2.301×10^5
							4	2.308×10^5
							6	3.452×10^5
							12	9.971×10^5
O	16.000	–	2.468×10^5	–	–	5	3	1.903×10^3
							1	2.717×10^3
							5	1.899×10^5
							1	4.044×10^5
							5	8.829×10^5
NO	30.008	2.45	8.990×10^4	1	2699.2	4	2	5.262×10^5
							4	5.496×10^5
C	12.011	–	7.116×10^5	–	–	1	3	1.962×10^2
							5	5.204×10^2
							5	1.219×10^5
							1	2.590×10^5
							5	4.036×10^5
CO_2	44.011	1.13	-3.933×10^5	2	960.1	1		
				1	1992.5			
				1	3380.2			
CO	28.011	2.78	-1.139×10^5	1	3082.0	1	6	5.824×10^5
							3	6.687×10^5
							6	7.453×10^5
							2	7.785×10^5
H_2	2.016	175.09	0.0	1	6100.0	1	1	1.097×10^6
							2	1.196×10^6
							3	1.352×10^6
H	1.008	–	2.110×10^5	–	–	1	3	9.839×10^5
							4	1.166×10^6
							5	1.230×10^6

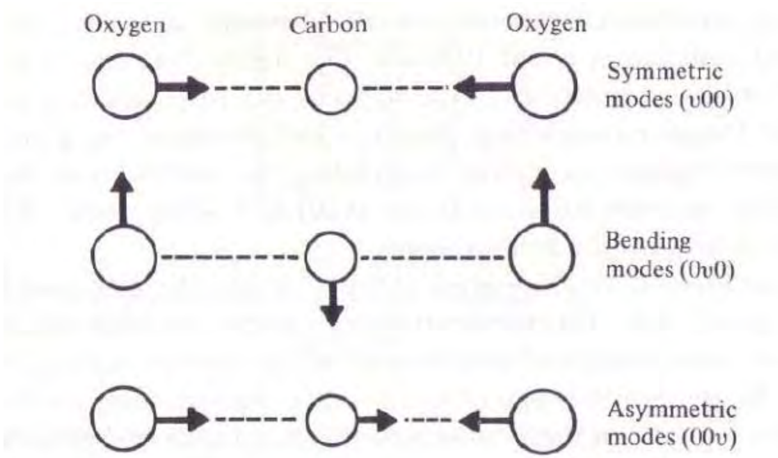

Dissociation temperatures

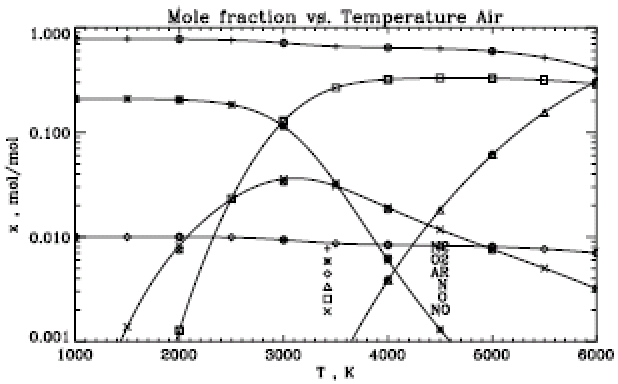

Air, $\rho = 0.01 \mathrm{kg/m^3}$

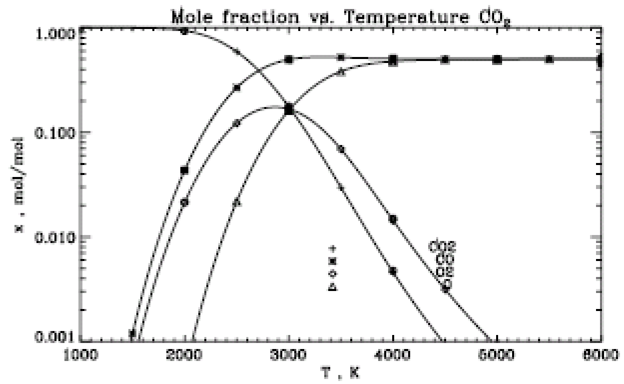

CO_2, $\rho = 0.01 \mathrm{kg/m^3}$

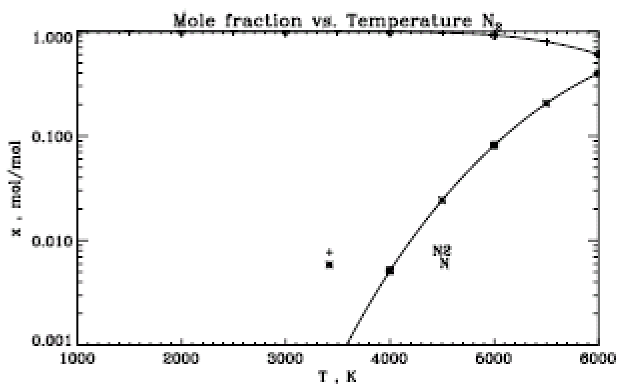

N_2, $\rho = 0.01 \mathrm{kg/m^3}$

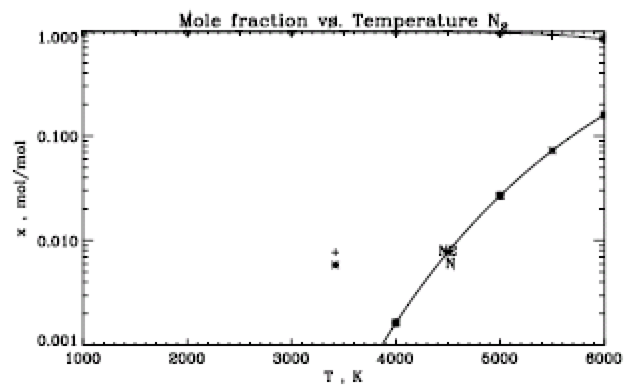

N_2, $\rho = 0.10 \mathrm{kg/m^3}$

St=q/rhoe*ue*(h0-0.5*ue^2*(1-r)-CpTw)

Detailed condition data (old shots)

Table A.1: Summary of freestream conditions for all shots.

Shot	P_0 $[MPa]$	T_0 $[K]$	h_0 $[MJ/kg]$	P_∞ $[kPa]$	T_∞ $[K]$	ρ_∞ $[kg/m^3]$	U_∞ $[m/s]$	M_∞ $[-]$
2331	52.2	7375	10.75	21.8	1487	4.92×10^{-2}	4286	5.6
2332	51.2	7095	10.90	22.8	1569	4.96×10^{-2}	4211	5.4
2333	50.0	4434	9.43	40.9	2214	8.69×10^{-2}	3248	4.3
2334	50.1	5380	10.89	32.8	1980	6.29×10^{-2}	3799	4.7
2335	37.6	3459	5.58	27.7	1426	9.86×10^{-2}	2647	4.6
2336	37.2	3606	6.12	27.8	1532	9.12×10^{-2}	2741	4.6
2337	51.2	7379	11.37	23.2	1662	4.74×10^{-2}	4338	5.4
2433	39.1	5305	8.34	17.9	1250	5.00×10^{-2}	3712	5.4
2434	42.5	5538	8.87	20.3	1369	5.17×10^{-2}	3816	5.3
2435	48.9	5843	9.53	24.5	1522	5.60×10^{-2}	3942	5.2
2436	49.5	6069	10.07	25.7	1659	5.39×10^{-2}	4040	5.1
2437	46.8	6567	11.33	27.3	2178	4.37×10^{-2}	4363	4.8
2438	48.9	6069	10.08	25.5	1660	5.35×10^{-2}	4040	5.1
2439	55.5	5715	9.15	26.6	1423	6.51×10^{-2}	3873	5.3
2440	53.8	5216	7.99	25.1	1182	7.39×10^{-2}	3643	5.4
2441	52.6	4689	7.33	27.7	1285	8.05×10^{-2}	3407	5.1
2442	53.3	4250	7.18	33.0	1479	8.94×10^{-2}	3291	4.8
2443	53.9	3702	4.38	36.3	1448	1.13×10^{-1}	2938	4.7
2444	53.0	3616	5.99	40.3	1560	1.31×10^{-1}	2740	4.5
2445	53.3	3782	6.61	40.4	1674	1.21×10^{-1}	2834	4.5
2446	55.8	4742	6.85	22.4	931	8.36×10^{-2}	3384	5.7
2447	50.5	4357	6.06	18.9	783	8.43×10^{-2}	3193	5.8
2448	48.4	4358	6.07	18.0	783	8.01×10^{-2}	3193	5.8
2449	45.7	4286	5.94	17.1	762	7.84×10^{-2}	3164	5.8

Preliminary Results with Porous Injector

Control Experiment – Smooth Surface

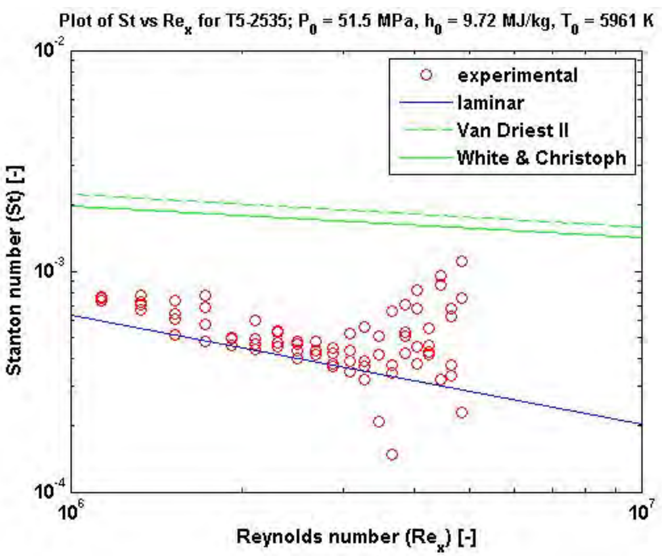

Porous injector design looks very promising

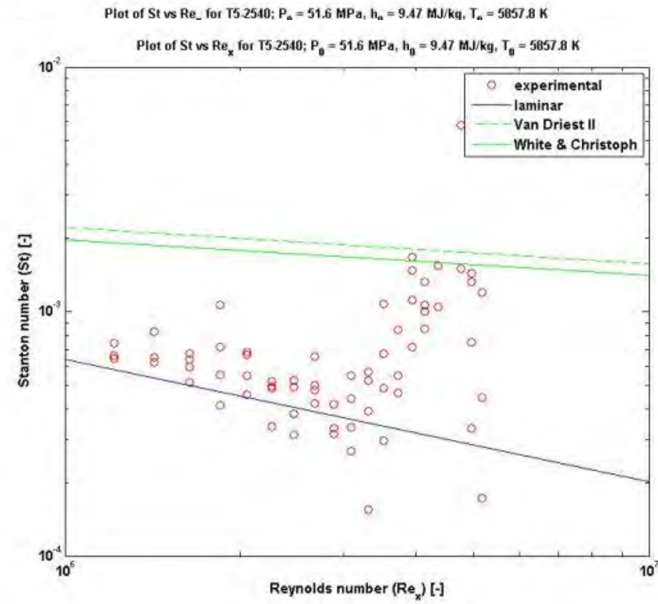

orous Injector – no flow

oundary layer not disturbed

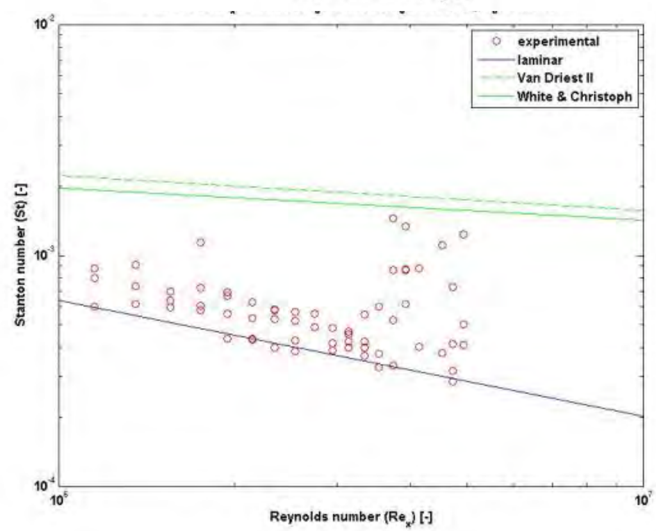

Preliminary data with porous injector and 20 psi CO_2 run tank pressure

Boundary layer not disturbed

CO_2 Injection System

The injection of CO_2 is triggered by a proximity switch sensing the recoil of T5, ~100 ms before flow begins in the test section

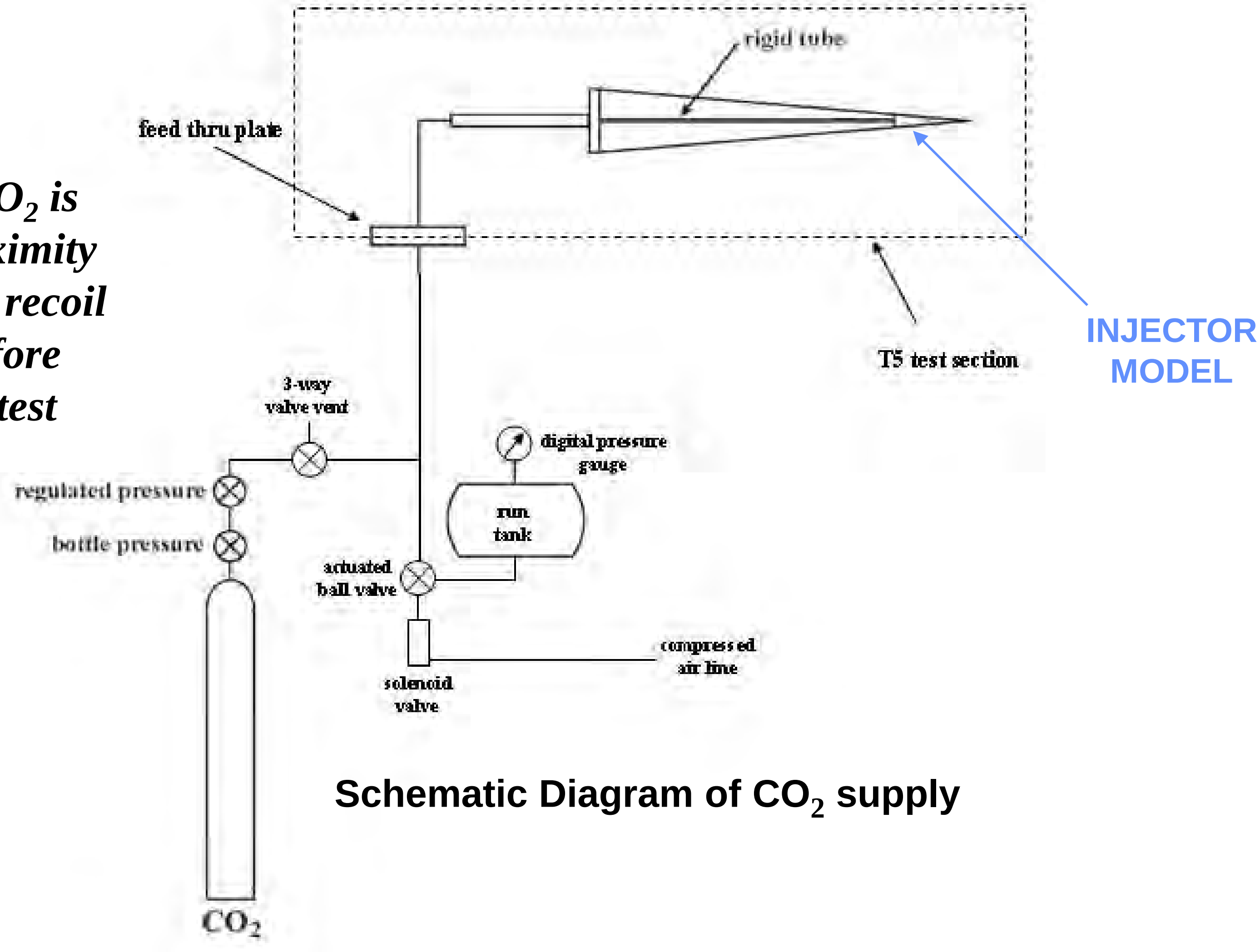

Schematic Diagram of CO_2 supply

Experimental model

Injector section installed in ~1m long, 5-degree half angle cone

Preliminary Results (10 MJ/kg)

Control Experiment – Smooth Surface

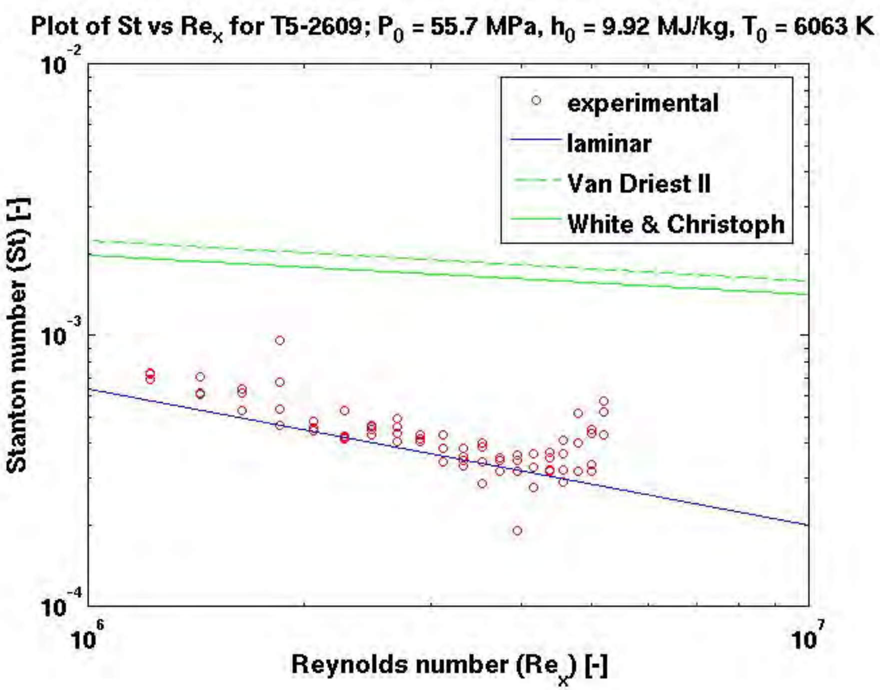

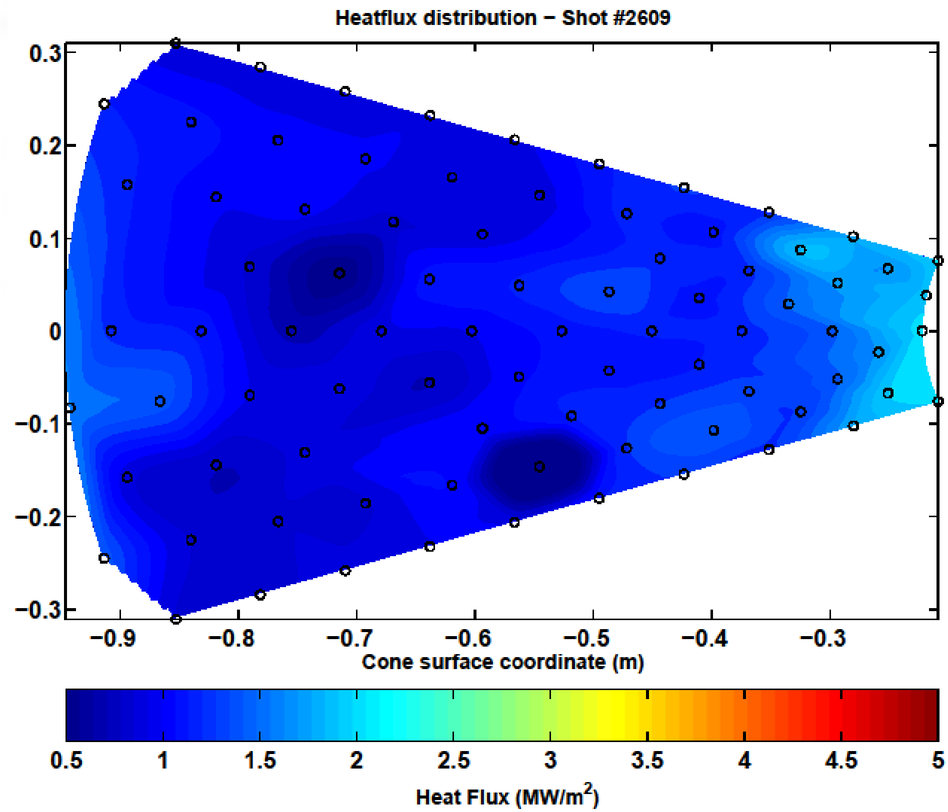

Initially laminar flow

Re_{tr} = 4.36 x 10^6

Four rows of orifices

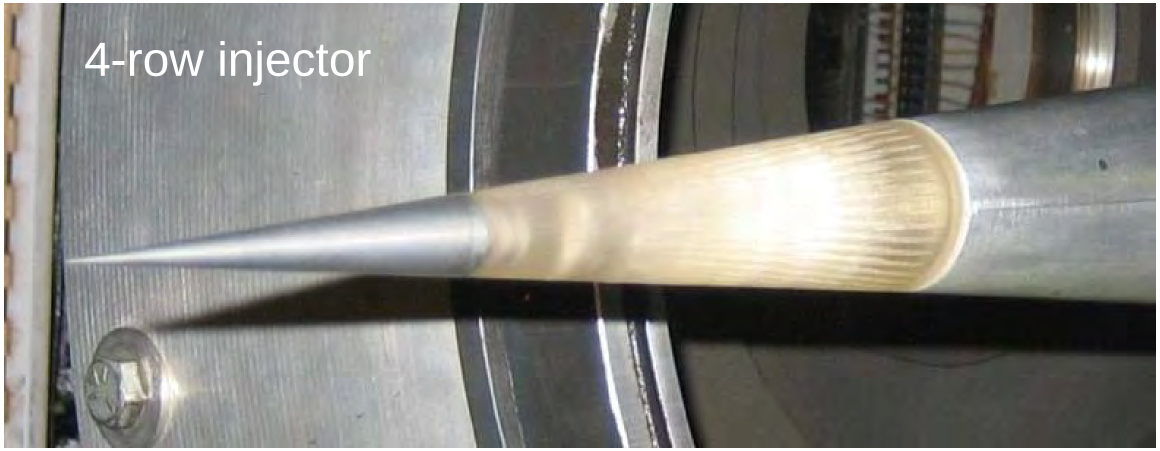

Injector with four rows of orifices, installed in T5 test section

Preliminary Results

Four-Row Injector (CO2 injection at 26.0 grams/sec)

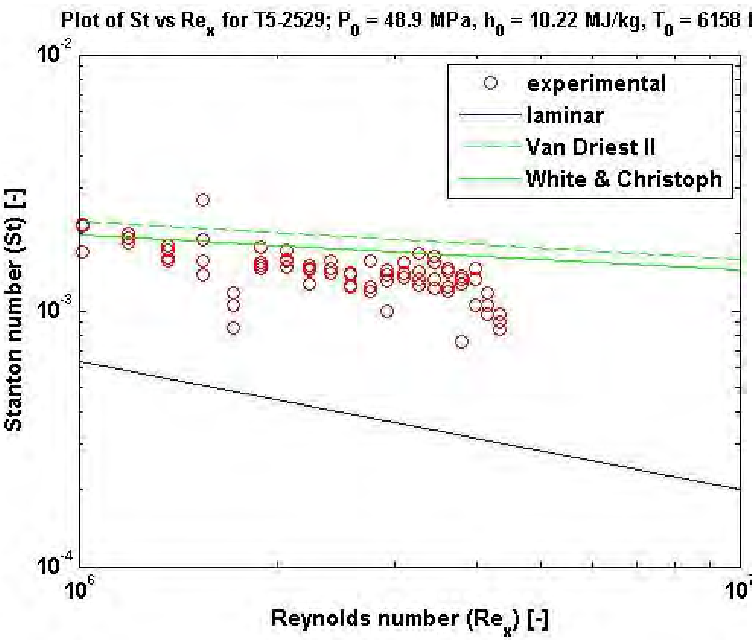

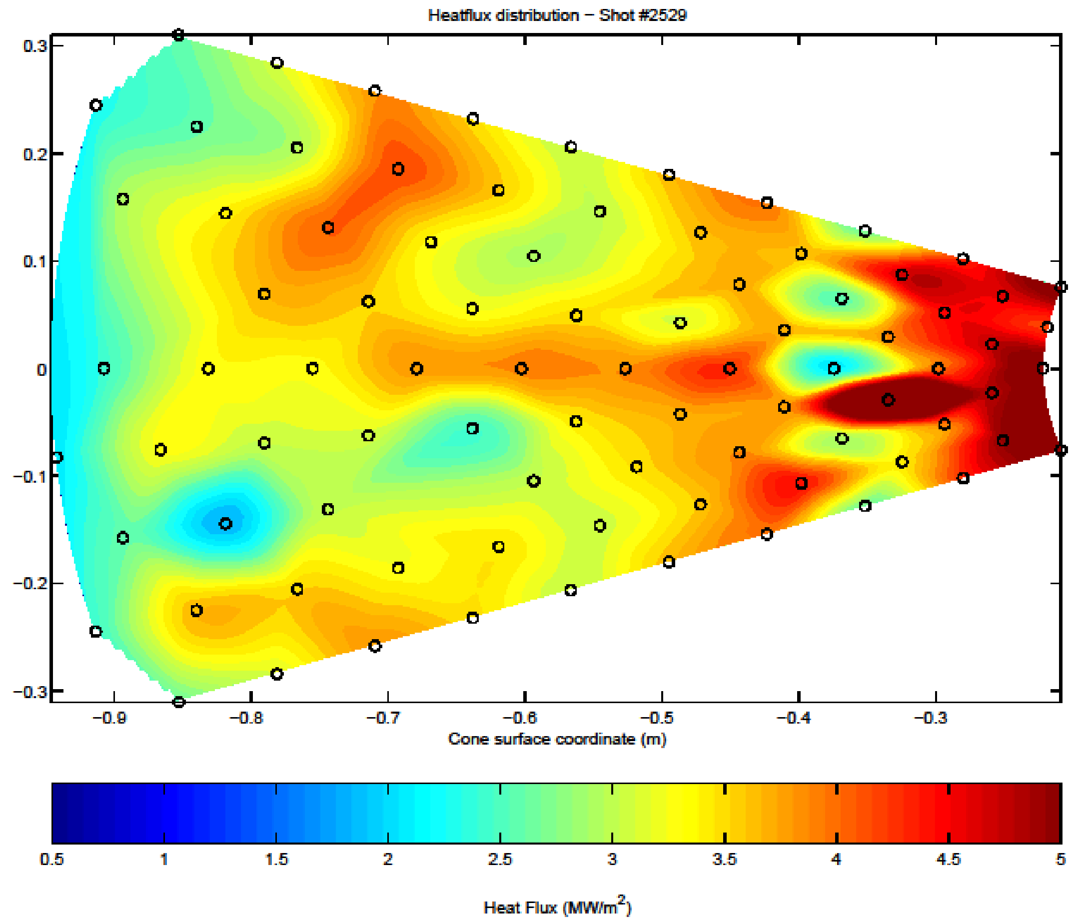

Immediate Transition

Preliminary Results

Four-Row Injector (no injection)

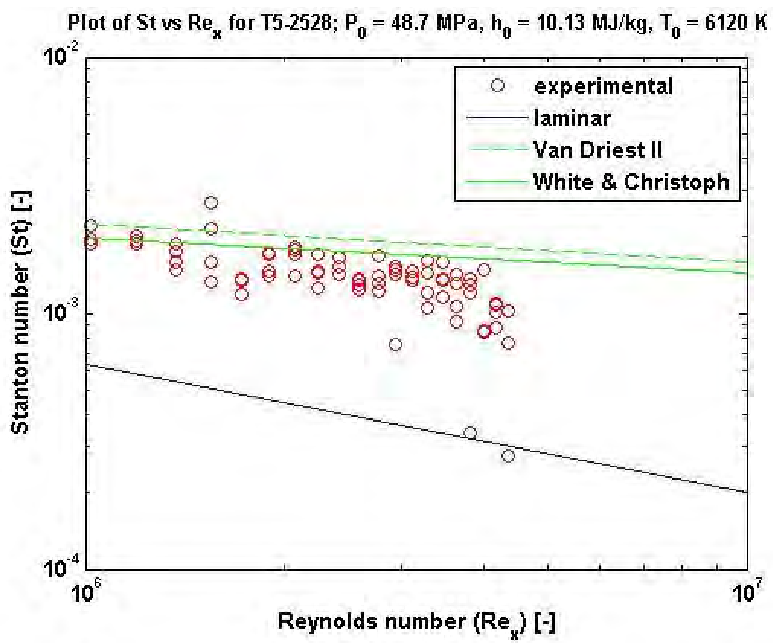

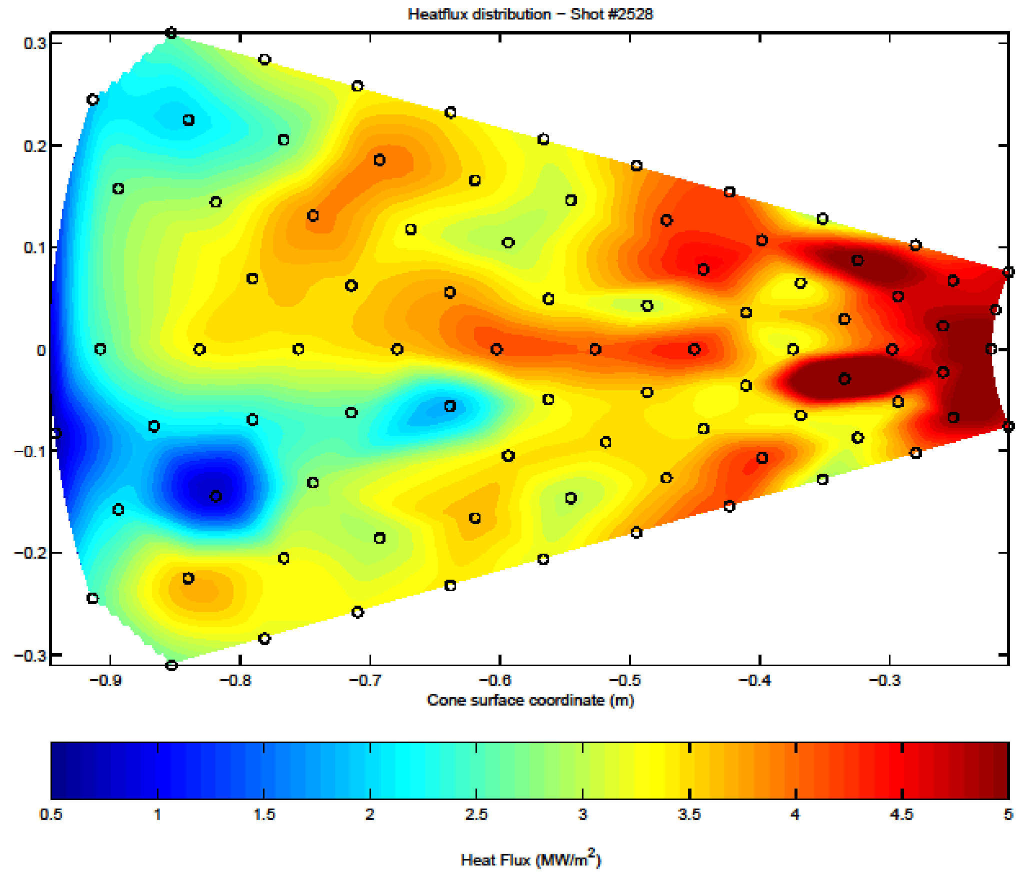

Immediate Transition

One row injector

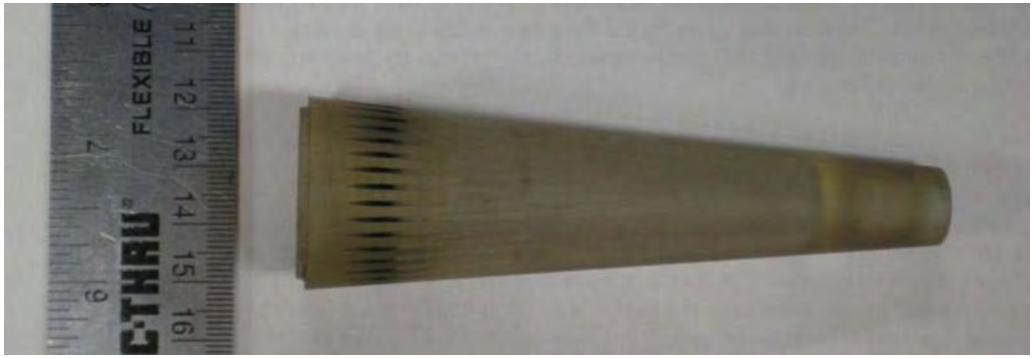

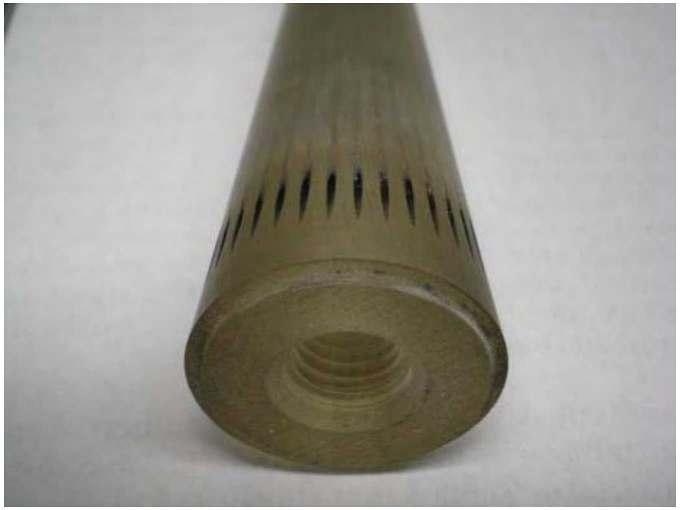

One row of orifices

Preliminary Results

One-Row Injector (no injection)

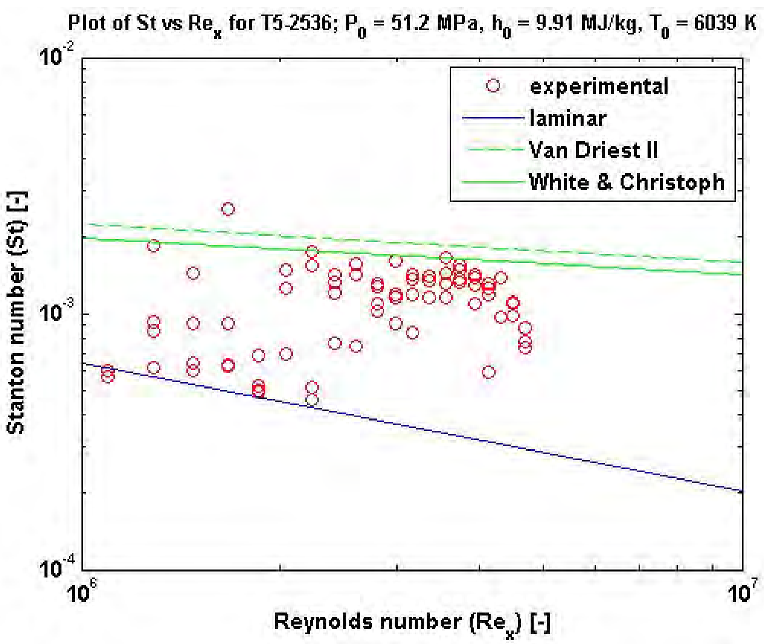

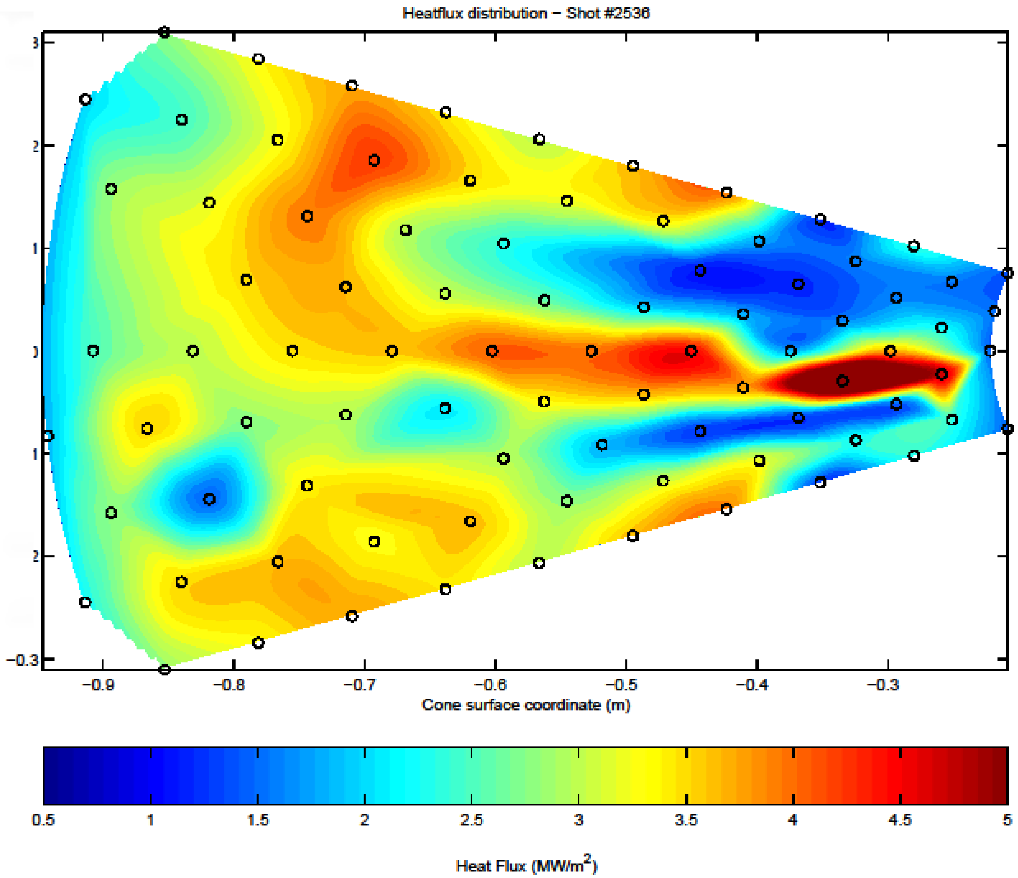

Transition (though not immediately full turbulence)

T profile and N factor for high and low enthalpy conditions

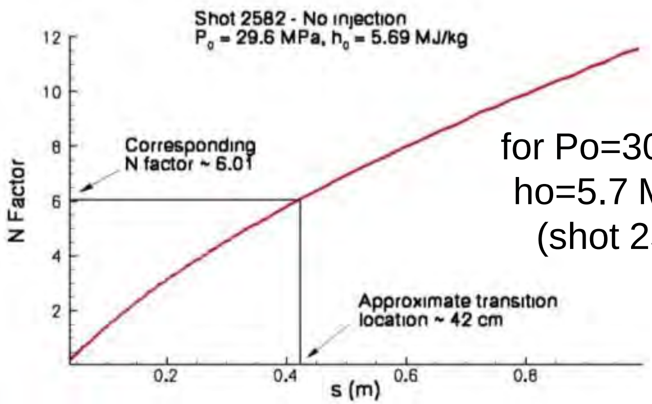

for Po=30MPa,
ho=5.7 MJ/kg
(shot 2582)

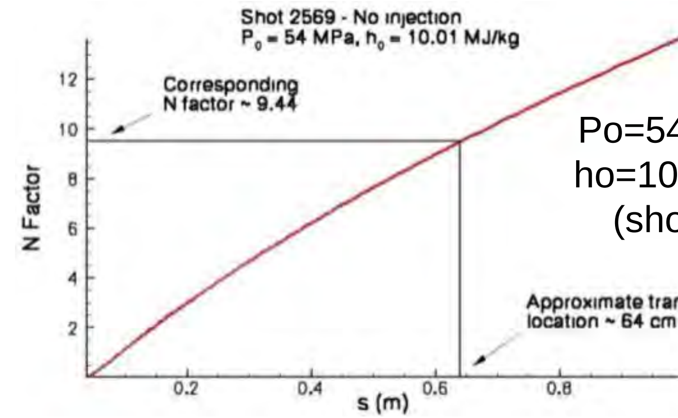

Po=54MPa,
ho=10 MJ/kg
(shot 2569)

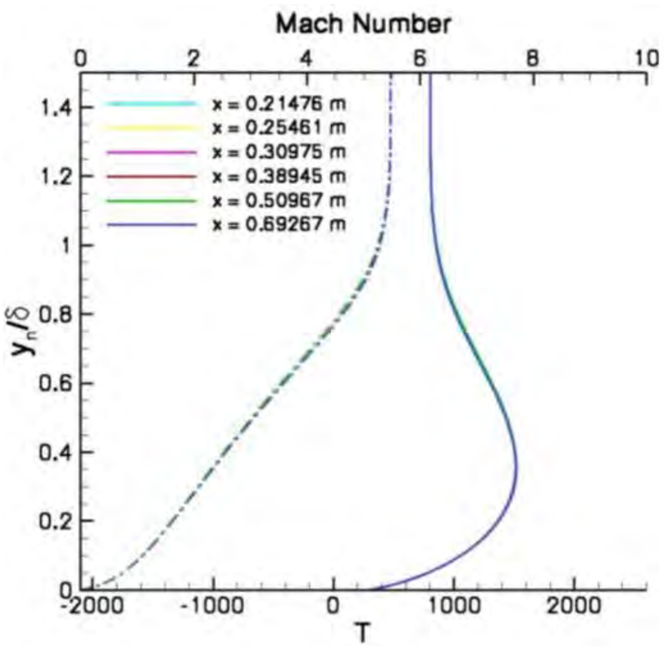

T : solid line
M : dash dot line

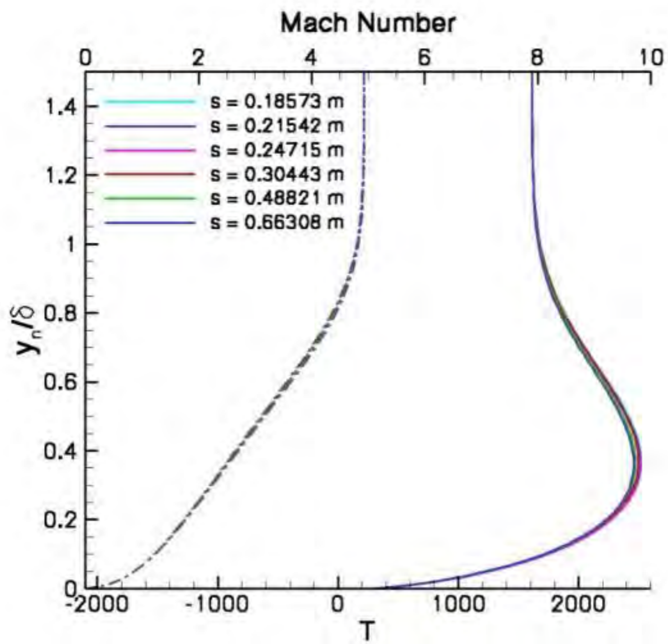

N2 results

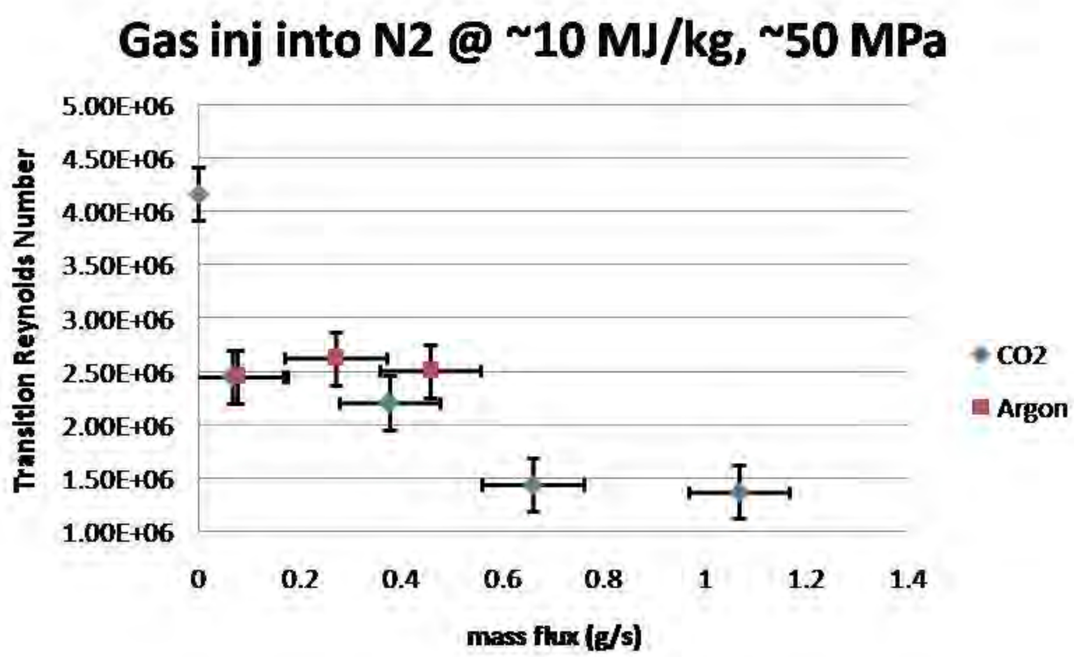

Gas inj into N2 @ ~10 MJ/kg, ~50 MPa
Transition Reynolds Number
5.00E+06
4.50E+06
4.00E+06
3.50E+06
3.00E+06
2.50E+06
2.00E+06
1.50E+06
1.00E+06
0
0.2
0.4
0.6
0.8
1
1.2
1.4
mass flux (g/s)
CO2
Argon

Porous Injector Results (10 MJ/kg)

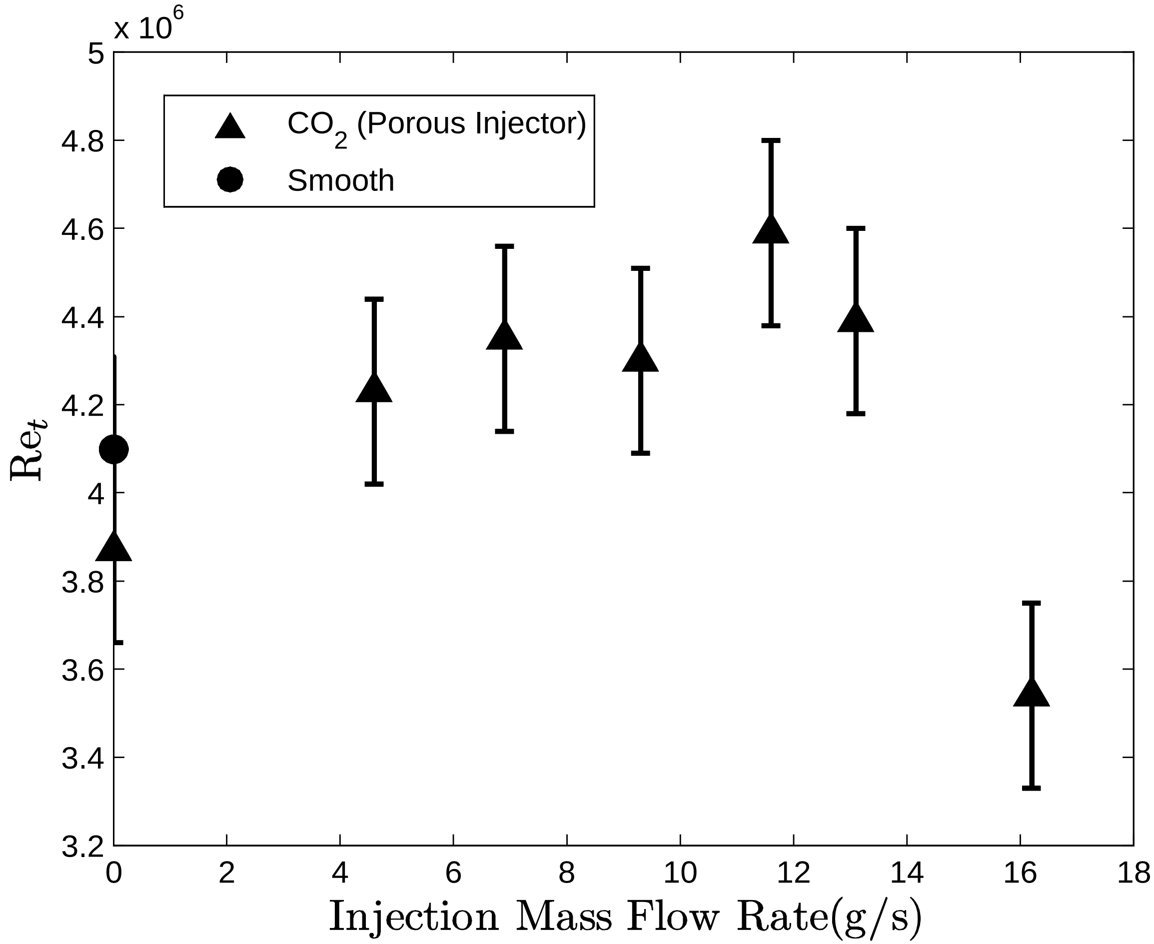

Summary of results (intermittency method)

Porous Injector Results 1/2